Bioorganic Chemistry 92 (2019) 103222

Contents lists available at ScienceDirect

Bioorganic Chemistry

journal homepage: www.elsevier.com/locate/bioorg

Synthesis, biological evaluation and *in silico* modelling studies of 1,3,5-trisubstituted pyrazoles carrying benzenesulfonamide as potential anticancer agents and selective cancer-associated hCA IX isoenzyme inhibitors

Cem Yamali[a], Halise Inci Gul[a,*], Abdulilah Ece[b], Silvia Bua[c], Andrea Angeli[c], Hiroshi Sakagami[d], Ertan Sahin[e], Claudiu T. Supuran[c]

[a] Department of Pharmaceutical Chemistry, Faculty of Pharmacy, Ataturk University, Erzurum, Turkey
[b] Department of Pharmaceutical Chemistry, Faculty of Pharmacy, Biruni University, Istanbul, Turkey
[c] Neurofarba Department, Sezione di Scienza Farmaceutiche e Nutraceutiche, Universita degli Studi di Firenze, Via U. Schiff 6, 50019 Sesto Fiorentino (Florence), Italy
[d] Meikai University Research Institute of Odontology (M-RIO), Sakado, Saitama 350-0283, Japan
[e] Department of Chemistry, Faculty of Science, Ataturk University, Erzurum, Turkey

ARTICLE INFO

Keywords:
Pyrazole
Carbonic anhydrase
hCA IX
Cytotoxicity
Anticancer
Sulfonamide
Molecular modelling

ABSTRACT

Inhibition of carbonic anhydrases (CAs, EC 4.2.1.1) has clinical importance for the treatment of several diseases. They participate in crucial regulatory mechanisms for balancing intracellular and extracellular pH of the cells. Among CA isoforms, selective inhibition of hCA IX has been linked to decreasing of cell growth for both primary tumors and metastases. The discovery of novel CA inhibitors as anticancer drug candidates is a current topic in medicinal chemistry. 1,3,5-Trisubstituted pyrazoles carrying benzenesulfonamide were evaluated against physiologically abundant cytosolic hCA I and hCA II and trans-membrane, tumor-associated hCA IX isoforms by a stopped-flow CO_2 hydrase method. Their *in vitro* cytotoxicities were screened against human oral squamous cell carcinoma (OSCC) cell lines (HSC-2) and human mesenchymal normal oral cells (HGF) *via* 3-(4,5-Dimethylthiazol-2-yl)-2,5-Diphenyltetrazolium Bromide (MTT) test. Compounds 6, 8, 9, 11, and 12 showed low nanomolar hCA II inhibitory potency with Ki < 10 nM, whereas compounds 9 and 12 displayed Ki < 10 nM against hCA IX isoenzyme when compared with reference Acetazolamide (AZA). Compound 9, 4-(3-(hydrazinecarbonyl)-5-(4-nitrophenyl)-*1H*-pyrazol-1-yl)benzenesulfonamide, can be considered as the most selective hCA IX inhibitor over off-target cytosolic isoenzymes hCA I and hCA II with the lowest Ki value of 2.3 nM and selectivity ratios of 3217 (hCA I/hCA IX) and 3.9 (hCA II/hCA IX). Isoform selectivity profiles were also discussed using *in silico* modelling. Cytotoxicity results pointed out that compounds 5 (CC_{50} = 37.7 μM) and 11 (CC_{50} = 58.1 μM) can be considered as lead cytotoxic compounds since they were more cytotoxic than 5-Fluorouracil (5-FU) and Methotrexate (MTX).

1. Introduction

Inhibition of carbonic anhydrases (CAs, EC 4.2.1.1) has clinical importance for the treatment of several diseases such as glaucoma, epilepsy, obesity, and gastric ulcers [1–3]. More recently, numerous studies reported that CA inhibition has an important role in cancerogenesis and tumor metastasis [4–7]. CAs are metalloenzymes present in all living organisms which are necessary for CO_2 hydration to bicarbonate and protons. They participate in crucial regulatory mechanisms for balancing intracellular and extracellular pH of all cells [8].

Main classes of CA inhibitors (CAIs) are comprised of primary sulfonamides and their bioisosteres such as sulfamates, sulfamides, etc., which bind to the Zn^{+2} ion of the enzyme to generate a tetrahedral adduct as zinc-binding groups. Furthermore, their scaffolds participate in other favorable molecular interactions with amino acid residues located in the active site of the enzyme [9]. Using of CAIs for medical applications draws attention due to the large distribution of CA isoforms within different tissues as well as on their involvement in many physiological/pathological conditions [1]. Among these isoenzymes, the selective inhibition of cancer-associated hCA IX and hCA XII has

* Corresponding author at: Ataturk University, Faculty of Pharmacy, Department of Pharmaceutical Chemistry, 25240 Erzurum, Turkey.
E-mail address: incigul1967@yahoo.com (H.I. Gul).

https://doi.org/10.1016/j.bioorg.2019.103222
Received 1 May 2019; Received in revised form 16 August 2019; Accepted 26 August 2019
Available online 28 August 2019

Table 1
CA inhibitory potency of the well-known CAIs in clinical use [16].

Ki				
Compound	hCA I (μm)	hCA II (nM)	hCA IX (nM)	hCA XII (nM)
AZA	0.25	12	25	5.7
MZA	0.05	14	27	3.4
EZA	0.025	8	34	22
DCP	1.20	38	50	50
DZA	50	9	52	3.5
BRZ	45	3	37	3.0
IND	0.031	15	24	3.4

anticancer effects leading to decreasing of growth for both primary tumors and metastases [10]. In particular, hCA IX is expressed in a limited number of normal tissues, while its overexpression is observed on the cell surface of a large number of solid tumors [10–12]. Previous studies revealed that CAIX is over expressed in different human cancers such as breast, kidney, rectum, ovarian, esophagus, cervix, uterine, lung, and head [13].

The selectivity of the clinically used inhibitors or compounds designed for various isoforms is important to target a specific or a certain disease without undesired side effects [14]. Selective inhibition of hCA IX isoenzyme is required for the treatment of cancer without side effects which would result from the inhibition of other widespread hCA isoforms, such as the cytosolic hCA II enzyme [1,12,15].

Well-known first and second generation CAIs as clinically used drugs such as acetazolamide (AZA), methazolamide (MZA), ethoxzolamide (EZA), dichlorophenamide (DCP), dorzolamide (DZA), brinzolamide (BRZ), and indisulam (IND) were presented in Table 1 with their CA inhibitory results against hCA I, hCA II, hCA IX and hCA XII isoenzymes [16]. The standard CA inhibitors given in Table 1 had Ki value of 24–52 nM against hCA IX while Ki values of the some drugs towards hCA II is in the range of 3–38 nM [16].

Even if popular primary sulfonamides have inhibitory potency against the target isoenzymes, still they have no desirable selectivity profile. Thus, the critical issue for designing novel CAIs is to obtain CA isoenzyme selective candidates against target enzymes for the desired bioactivity in order to decrease side effects in addition to physicochemical problems such as poor water solubility of the sulfonamides [17].

Despite sulfonamide derivatives are effective CAIs, most of them do not have isoform selectivity against tumor related isoforms CA IX and CA XII. Additionally, similarities of the active side of the isoforms mentioned effect specificity of CAIs. This situation is particularly considered in the case of CA II isoform which has the broadest distribution in body cells such as red blood cells. It was also expressed that as many drugs are delivered systemically and membrane permeable, it is possible that CA II isoform cannot allow reaching of drugs as CAIs within cancer cells and also CAIs show limited efficacy and selectivity against CA IX and CA XII isoforms [18].

In an attempt to overcome selectivity problems, atypical zinc chelating scaffolds besides primary sulfonamides were also offered as remarkable CA inhibitors such as dithiocarbamates, hydroxamates, phenols, polyamines, coumarins, benzoic acid derivatives, secondary/tertiary sulfonamides with various chemical differences in their pharmacophoric moieties [19]. Additionally, many efforts have been also made to explore chemical modifications of the CAIs structures that could have a positive affect on lack of selectivity and water solubility problems. For this purpose, amino acids, peptides or their hybrids for designing CAIs which could provide a solution to the problems have applied [17].

Mollica et al. [20] reported the effects of novel probenecid-based amide derivatives obtained with natural L-amino acids and tertiary sulfonamide (Probenecid) against hCA I, II, IX, and XII isoforms. Most of them presented a complete loss of hCA II inhibition (Kis > 10.000 nM) and strong inhibitory activity against hCA IX and XII in the nanomolar range. The transformation of the COOH group into $CONH_2$ was also interesting, resulting in a remarkably lower affinity against the off-target hCA II. This study also provides useful information about the application of the amino acid tail approach to an atypical zinc-chelating molecule [20].

SLC-0111 and indisulam (E7070) compounds were found promising CAIs in clinical trials for the treatment of tumors among the wide range of sulfonamide type compounds evaluated as potential anticancer agents. Phase I clinical trials of SLC-0111 for tumors overexpressing hCA IX were completed and phase II clinical trials will be scheduled in the near future [21–23]. E7070, another primary sulfonamide was developed as an antineoplastic agent and reached phase II clinical trials, which have been stopped however in 2014 [24,25].

Khloya et al. [26] reported 1,3-diaryl pyrazole bearing sulfonamide as potent inhibitors of the tumor-associated carbonic anhydrase isoforms. Some compounds tested displayed affinity for hCA IX (Ki < 5 nM) at low nanomolar while the others had Ki value lower than < 10 nM against hCA XII. The compounds presented in Fig. 1 were reported as potent CA inhibitors with their impressive results towards hCA I, hCA II, hCA IX, hCA XII in designing novel, potent, and selective CAIs [26].

More recently, Pazopanib, a drug carrying a primary sulfonamide moiety was approved by FDA as an anticancer agent which is a multitarget tyrosine kinase inhibitor used clinically for the treatment of different tumors [27–29]. Its bioactivity was also associated with the inhibition of the carbonic anhydrase enzyme as well as kinase inhibition potency [30]. Winum et al. [31] reported CA inhibitory potencies of Pazopanib against the catalytically active several CA isoforms such as hCA I, hCA II, hCA IX and hCA XII. Some of the results reported in the literature are in Table 2. The results reveal that Pazopanib showed excellent CA inhibitory activity towards cancer-related isoenzymes hCA IX (Ki = 9.1 nM) and hCA XII (Ki = 0.88 nM) [31]. According to these data, it was estimated that in addition to the tyrosine kinase inhibitor action, Pazopanib may show its antitumor/antimetastatic effects due to the potent inhibition of the tumor-associated, hypoxia-inducible enzymes hCA IX and hCA XII [31].

A large number of pyrazoles and its derivatives that exhibit

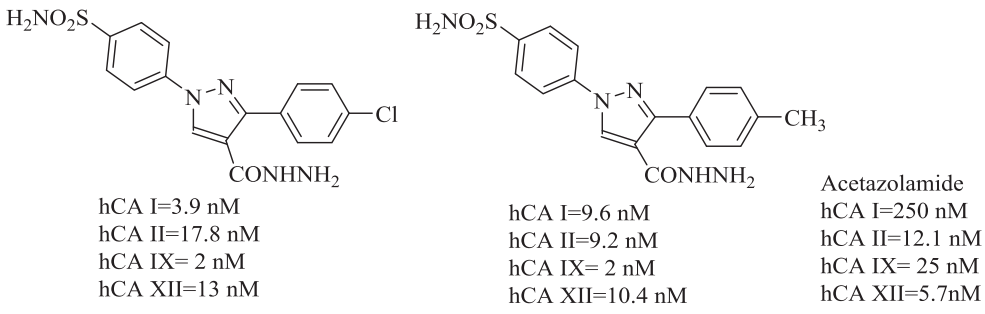

Fig. 1. 1,3-Diarylpyrazole derivatives reported in the literature [26] as potent hCA IX and hCA XII inhibitors.

Table 2
CA inhibitory potency of the anticancer drug Pazopanib [31].

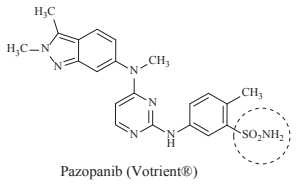

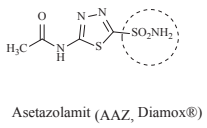

	Ki (nM)	
	AAZ	Pazopanib
hCA I	250	12.1
hCA II	12	32.4
hCA IX	25	9.1
hCA XII	5.7	0.88

remarkable pharmacological activities are known as a group of very active heterocyclic compounds [32,33]. Currently, some of them are in clinical use such as Celecoxib, Ruxolitinib, and Crizotinib (Fig. 2). Celecoxib is a COX-2 inhibitor approved by the FDA for the treatment of rheumatoid arthritis and osteoarthritis [34,35]. According to data reported, the compound also reduces prostate tumors in experimental models by affecting cell cycle regulation [36]. Additionally, it was reported that COX-2 promotes tumor-specific angiogenesis, inhibits apoptosis, and induces proangiogenic factors such as VEGF [37]. Celecoxib can also be considered as a representative compound of pyrazole containing diaryl substituted heterocyclic template in pharmaceutical chemistry. Moreover, Ruxolitinib and Crizotinib carrying pyrazole moiety are also used as antitumor agents in the clinic for the treatment of myeloproliferative neoplasm and non-small cell lung carcinoma, respectively [38,39].

Considering the exciting promising literature survey on primary sulfonamide and pyrazole pharmacophores, and approved drugs carrying sulfonamide and pyrazole moieties which are in clinical use for treatment of cancer, in the present study, it was aimed to synthesize 1,3,5-trisubstituted pyrazoles carrying benzenesulfonamide, evaluation of their CA inhibition properties towards hCA I, hCA II, and hCA IX isoenzymes, and also their cytotoxicities against OSCC cell lines (HSC-2 and HGF) to find out potential drug candidate/s. In an attempt to explore selectivity profiles for hCA IX versus hCA I and II, we also planned *in silico* modelling studies for the lead compound of this study. Target compounds were derivatized by changing aryl parts as phenyl, 4-methyl phenyl, 4-nitro phenyl and 2-thienyl on the 5th position of pyrazole. In addition, insertion of ester and hydrazide groups on the 3th position of the core ring pyrazole were considered as a second modification to obtain target compounds (Fig. 2).

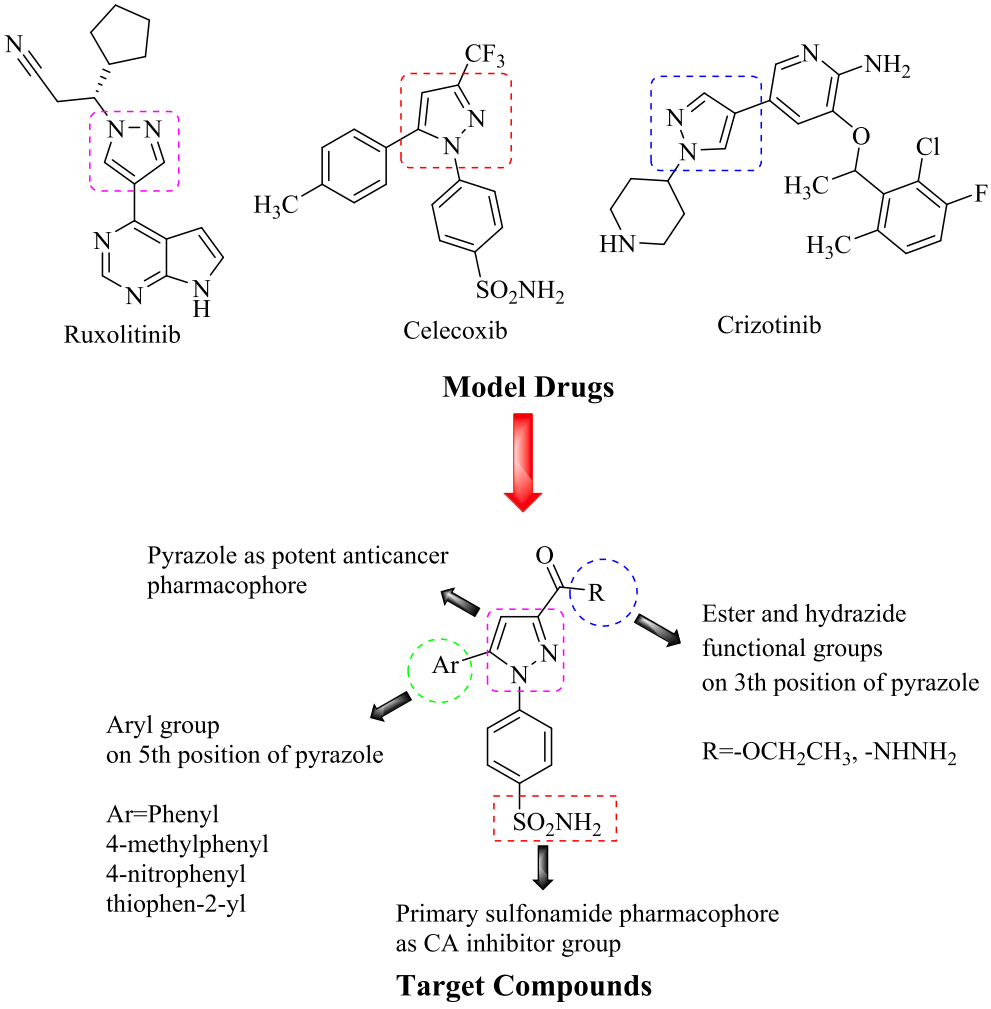

Fig. 2. Chemical structure of anticancer drugs and rationally designed template for anticancer drug candidate compounds targeting for CA IX isoenzyme inhibition.

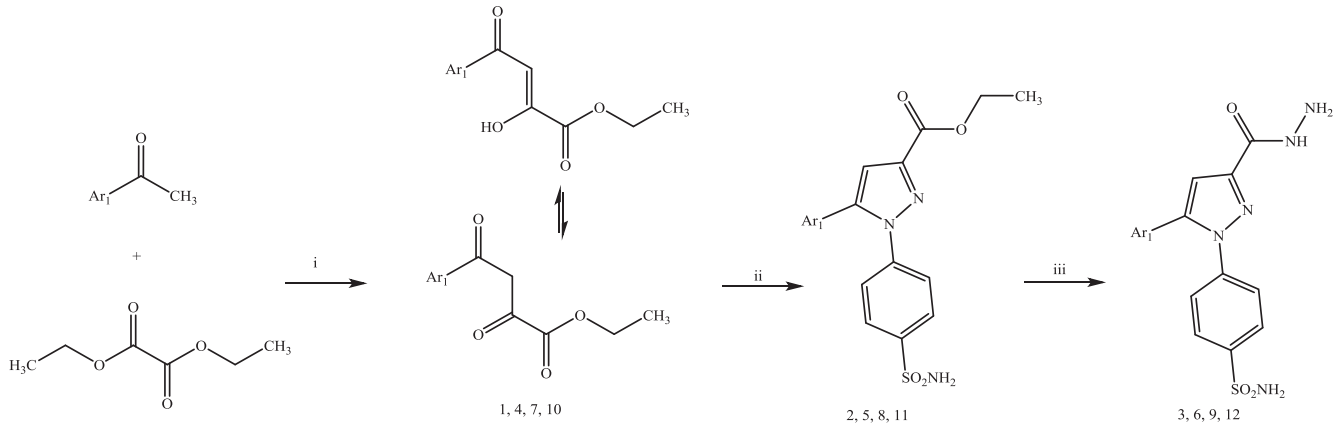

Scheme 1. Synthetic pathway of the compounds 1,3,5-trisubstituted pyrazoles carrying benzenesulfonamide. (i) NaOEt, EtOH or THF, ice bath, and rt. (ii) 4-Hydrazinobenzenesulfonamide.HCl, EtOH, reflux. (iii) Hydrazine hydrate, EtOH, reflux. Ar_1 = Phenyl (1–3), 4-Methyl phenyl (4–6), 4-Nitro phenyl (7–9), Thiophen-2-yl (10–12).

2. Results and discussion

2.1. Chemistry

The synthetic route to obtain 1,3,5-trisubstituted pyrazole carrying benzenesulfonamide is presented in Scheme 1. Claisen condensation of the suitable aryl ketones with diethyl oxalate in the presence of sodium ethoxide gave ethyl 2,4-dioxo-4-arylbutanoates derivatives with the yield 1 (50%), 4 (54%), 7 (89%), 10 (50%). The cyclization of β-diketones (1, 4, 7, 10) with 4-hydrazinobenzenesulfonamide hydrochloride by refluxing in ethanol gave ethyl 5-aryl-1-(4-sulfamoylphenyl)-*1H*-pyrazole-3-carboxylate derivatives in excellent yield [2 (71%), 5 (91%), 8 (89%), 11 (80%)]. As a final step, 1,5-diarylpyrazole ethyl esters were then reacted with hydrazine hydrate to afford 4-(3-(hydrazinecarbonyl)-5-aryl-*1H*-pyrazol-1-yl) benzenesulfonamide derivatives with the good yield 3 (90%), 6 (51%), 9 (81%), 12 (86%) by refluxing in ethanol.

The chemical structure of the compounds was confirmed by NMR spectra and HRMS analysis (See Supplementary file for spectra). According to ^{1}H NMR data, chemical structures of the 2,4-dioxo-4-arylbutanoates derivatives (1, 4, 7, 10) were established to exist in an enol form. ^{1}H NMR spectra of the compounds 1 and 4 showed broad singlet signal of enol proton at δ 15.30 and 14.80 ppm, except 7 and 10. On the other hand, a signal belongs to alkene's proton for the four intermediates was shown at δ 7.09–6.91 ppm. Moreover, the spectrum of the compounds showed a couple of signal of aliphatic protons at δ 4.39–4.34 ppm (q, $-CH_2-$) and δ 1.42–1.39 ppm (t, $-CH_3-$).

The ^{1}H NMR spectra of ethyl 5-aryl-1-(4-sulfamoylphenyl)-*1H*-pyrazole-3-carboxylate derivatives (2, 5, 8, 11) showed the characteristic signal of H-4 of the pyrazole ring in the region δ 7.35–7.05 ppm as a singlet. A signal of sulfonamide group in the compounds also appeared in the range δ 7.56–7.44 ppm as a singlet or one within the other aromatic peaks. In the current study, 1,5-diaryl pyrazoles were designed as target compounds. That is why the synthetic method mentioned above carried out to obtain 1,5-diarylpyrazole isomer. In general, the cyclization of β-diketones with hydrazine derivatives may give a mixture of 1,5- and 1,3-diarylpyrazole esters based on the reaction conditions [40]. In most cases, 1,5-diarylpyrazole regioisomers were generated by carrying out the reaction in the presence of the hydrochloride salt of the hydrazine derivatives in refluxing ethanol with the high yields [41].

In this study, separation of the 1,5-diarylpyrazole isomers as a target compounds were performed by crystallization to afford pure target compounds in the high yields as reported above. After purification of the 1,5-diarylpyrazole isomers, the exact chemical structure of the representative compound 2 was established by NOESY experiment (See supplementary file for spectra). The chemical structure of 4-(3-(hydrazinecarbonyl)-5-aryl-*1H*-pyrazol-1-yl) benzenesulfonamide derivatives (3, 6, 9, 12) was confirmed by their ^{1}H NMR spectra which revealed the disappearance of the proton signals of $-OCH_2CH_3$ group in addition to the appearance of the proton signals of $-NHNH_2$ group. A signal of the $-NH-$ group was seen in region δ 10.20–9.59 ppm as a singlet while a signal of $-NH_2$ group was seen around δ 4.48 ppm as a singlet. The other aromatic protons' peaks were observed at the expected values as expected. HRMS results were also confirmed chemical structure of the compounds in accordance with their proposed chemical structure in addition to their purity. According to HRMS results, differences of mass results between calculated and measured values were lower than the value of 0.4%. Differences in calculated and measured values were in the range of 0.0017–0.0008.

The structure of ethyl-5-phenyl-1-(4-sulfamoylphenyl)-1*H*-pyrazole-3-carboxylate (2) was characterized by X-ray diffraction analysis (Fig. 3). Compound 2 was crystallized as a white block and was solved in the monoclinic space group $P2_1/c$ with four molecules in the unit cell. The structure has phenyl and $-OCH_2CH_3$ groups at opposite positions of pyrazole core. Among these, there is a benzenesulfonamide unit. Deviation from planarity of the molecule is due to significant steric effects and intermolecular interactions. In the pyrazole heterocycle, the bond lengths of N3—C9 = 1.3334(3) Å and C8—C7 = 1.378(4) Å are in the range of typical single bond values. The bond lengths between sulphur and oxygen S1—O1 = 1.427(3) Å and S1—O2 = 1.436(3) Å falls within the double bond range. The crystal packing shows (Fig. 3) that molecules form centrosymmetric dimers connected by N1—H···O2 [$D\cdots A$ = 2.973(3)Å] hydrogen bonds. These dimeric units form a polymeric structure with adjacent molecules. The non-covalent C—H···O, N—H···C, and N—H···N interactions cause the formation of this polymeric form. The π-π stacking interactions between the delocalized π-electrons of the phenyl and pyrazole rings are relatively weak. Distance between rings centroids is in the range of 3.98–5.72 Å.

2.2. Carbonic anhydrase inhibition

In the present study, a small library of 1,5-diarylpyrazole benzenesulfonamides was evaluated against three human carbonic anhydrases such as physiologically abundant cytosolic hCA I and hCA II and trans-membrane, tumor-associated hCA IX isoforms by a stopped-flow, CO_2 hydrase assay method [42]. CA inhibition data is shown in Table 3. The results are expressed as Ki (inhibition constant, nM) values and the lowest Ki value indicates the best inhibitory potency of the compound against the corresponding isoenzyme. Acetazolamide (AZA) was used as a reference drug. Moreover, the selectivity ratio of the compounds for the inhibition of tumor-related CA IX over off-target cytosolic isoenzymes I and II was summarized in Table 4. The following results of

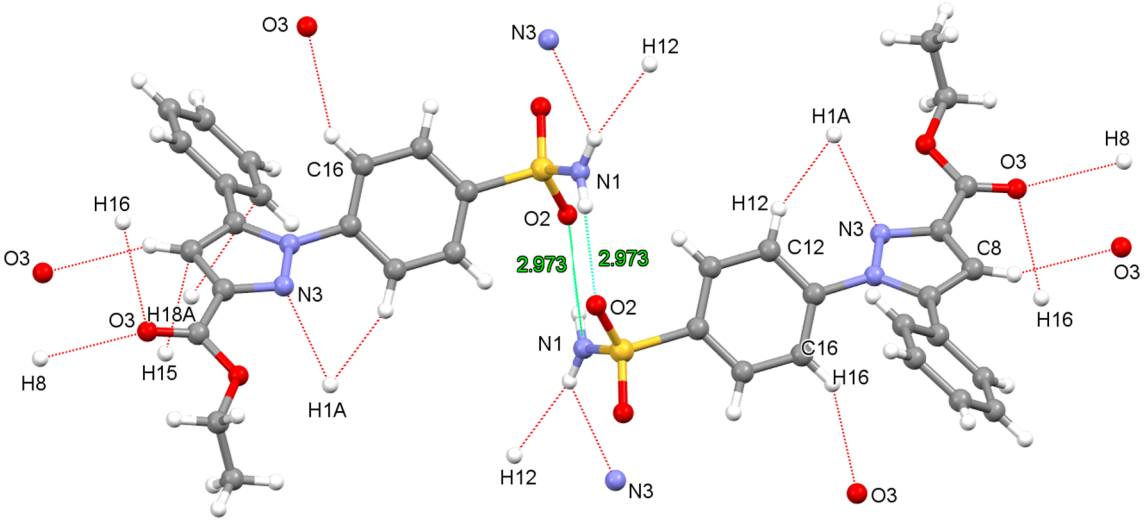

Fig. 3. Dimeric structure of molecule 2 with the short-contact interactions.

Table 3
Carbonic anhydrase inhibitory potency (Ki, nM) of the 1,3,5-trisubstituted pyrazoles carrying benzenesulfonamide towards hCA I, hCA II and hCA IX isoenzymes.

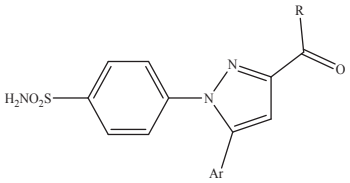

Ki (nM)					
Compound	Ar	R	hCA I	hCA II	hCA IX
2	Phenyl	OCH_2CH_3	47.1	60.9	225.3
3	Phenyl	$NHNH_2$	68.4	87.9	30.5
5	4-Methylphenyl	OCH_2CH_3	9176	86.1	175.8
6	4-Methylphenyl	$NHNH_2$	368.1	9.7	31.4
8	4-Nitrophenyl	OCH_2CH_3	6196	9.1	20.5
9	4-Nitrophenyl	$NHNH_2$	7399	8.9	2.3
11	Thiophen-2-yl	OCH_2CH_3	8.3	7.4	184.8
12	Thiophen-2-yl	$NHNH_2$	44.3	8.4	9.7
AZA			250	12.1	25.8

Table 4
Isoenzyme selectivity ratios of the compounds 1,3,5-trisubstituted pyrazoles carrying benzenesulfonamide.

	Selectivity ratio	
Compound	hCA I/hCA IX	hCA II/hCA IX
2	0.2	0.3
3	2.2	2.9
5	52.2	0.5
6	11.7	0.3
8	302	0.4
9	3217	3.9
11	0.04	0.04
12	4.6	0.9
AZA	9.7	0.5

the compounds tested against hCA I, hCA II and hCA IX were drawn from the data are presented in Tables 3 and 4.

i. The cytosolic hCA I isoenzyme was inhibited by the eight compounds bearing pyrazole-benzenesulfonamide pharmacophores (2, 3, 5, 6, 8, 9, 11, 12) with the inhibition constant (Ki) ranging between 8.3 − 9176 nM (hCA I), 7.4–87.9 nM (hCA II) and 2.3–225.3 nM (hCA IX) while reference drug AZA has Ki values of 250 nM, 12.1 nM and 25.8 nM towards hCA I, hCA II and hCA IX, respectively.
ii. Among the ethyl 5-aryl-1-(4-sulfamoylphenyl)-*1H*-pyrazole-3-carboxylate derivatives (2, 5, 8, 11), compound 11 carrying thiophene ring on the 5th position of pyrazole ring effectively inhibited hCA I isoenzyme with Ki value of 8.3 nM while 11 inhibited hCA I isoenzyme with Ki value of 7.4 nM. It showed that 11 was 30 times effective than AZA against hCA I and also it was 1.6 times more effective than AZA (Ki = 12.1 nM) against hCA II. On the other hand, the ester compound 8 was found as a good inhibitor among others with Ki value of 20.5 nM and its inhibitory potency was 1.3 times more than AZA (Ki = 25.8 nM) against hCA IX isoenzyme.
iii. When the inhibitory potencies of the 4-(3-(hydrazinecarbonyl)-5-aryl-*1H*-pyrazol-1-yl)benzenesulfonamide derivatives (3, 6, 9, 12) were considered against all isoenzymes, compound 12 against hCA I (Ki = 44.3 nM) and hCA II (Ki = 8.4 nM) and compound 9 against hCA IX (Ki = 2.3 nM) were found the best inhibitors. Among this type of compounds, compound 9 bearing 4-nitrophenyl ring was found highly effective for inhibiting tumor-associated hCA IX isoenzymes with the lowest Ki value of 2.3 nM. So, compound 9 showed approximately 11.2 times superior CA inhibition profile as compared to the reference AZA (Ki = 25.8 nM).
iv. When the hydrazide type compounds' inhibitory potencies were considered against tumor-associated hCA IX isoenzyme, it can be said that converting ethyl ester derivatives into hydrazide was found a useful modification to increase hCA IX inhibiting ability of the compounds. Interestingly, converting compound 11, ethyl ester derivative carrying thiophene ring, into hydrazide derivative 12 extremely increased the inhibitory potency more than 19 times towards hCA IX isoenzyme.
v. The data in Table 3 leads to the conclusion that 4-nitrophenyl bearing compounds (8 and 9) and thiophene bearing compounds (11 and 12) generally have good inhibitory profile against hCA II and hCA IX isoenzymes with the lowest Ki values among the compounds tested and also these compounds drawn attraction to design novel CA inhibitors. The results considered showed that the nature of the substituents present on the 5th position of pyrazole scaffold in terms of electron-withdrawing nitro group on phenyl

ring and bioisosteric replacement of phenyl ring by thiophene influenced CA inhibition profile positively.

vi. Overexpression of CA IX isoenzyme specifically in cancer cells makes it a good therapeutic target as a biomarker for cancer. The most important problem with the CAIs is the lack of selectivity towards a specific CA isoenzyme such as cancer-related hCA IX and hCA XII isoenzymes. Non-specific binding of clinically used CA inhibitors to other isoforms causes undesired side effects. One of the goals of this study is to obtain selective hCA IX inhibitors over the two major off-target CA isoenzymes as hCA I and hCA II. One of the challenges targeting hCA IX for the treatment of tumors is the structural similarity of hCA IX to hCA II isoenzyme. In fact, most isoforms of CAs have only a few differences in the active site of enzyme which makes it difficult for designing inhibitors that would specifically bind to one isoform over the others. The hCA I/hCA IX and hCA II/hCA IX ratios reveal that the isoenzyme selectivity of the compound against hCA IX isoenzyme as shown in Table 4. When selectivity ratios of the compounds tested were considered, some compounds make attraction towards cancer-associated hCA IX isoenzyme. Compounds 5 (5.4 times), 6 (1.2 times), 8 (31.2 times), 9 (331.7 times) were found more selective towards hCA IX over off-target isoenzyme hCA I while compounds 3 (5.8 times), 9 (7.8 times), and 12 (1.8) were found more selective towards hCA IX over off-target isoenzyme hCA II isoenzyme than reference drug AZA's isoform selectivity.

vii. On the other hand, we considered comparing CA inhibitory potency of 1,5-diaryl pyrazole with some 1,3-diaryl pyrazole towards hCA I, h CAII, and hCA IX isoenzymes to understand which kind of isomers can be considered for designing of novel and potent CA inhibitors. Khloya A. et al. reported pyrazole-4-hydrazinocarbonyl derivatives against hCA I, hCA II, hCA IX and hCA XII [26]. The inhibition data of compounds 4-(4-(hydrazinecarbonyl)-3-phenyl-*1H*-pyrazol-1-yl)benzenesulfonamide (6a), 4-(4-(hydrazinecarbonyl)-3-(p-tolyl)-*1H*-pyrazol-1-yl)benzenesulfonamide (6b) and 4-(4-(hydrazinecarbonyl)-3-(4-nitrophenyl)-*1H*-pyrazol-1-yl) benzenesulfonamide (6 g) are presented in Table 5. Compounds 6a (Ki = 2.8 nM)) and 6b (Ki = 2 nM) showed remarkably higher CA inhibition profile than AZA against hCA IX isoenzyme. Compound 6b bearing 4-methyl phenyl was found more effective with the lowest inhibition constant against hCA IX isoenzyme except for compound 6 g including 4-nitrophenyl derivative. On the other hand, according to present results reported by our group, compound 9 bearing 4-nitrophenyl ring was found highly effective for inhibiting tumor-associated hCA IX isoenyzme with the lowest Ki value of 2.3 nM among others. So, compound 9 showed approximately 11.2 times superior CA inhibition profile as compared to the reference AZA (Ki = 25.8 nM). It can be concluded that electron-withdrawing nitro substitution on the 5th position of the phenyl ring in 1,5-diarylpyrazole was useful modification to increase CA activity while the introduction of an electron-releasing group such as methyl on 3rd position in 1,3-diaryl pyrazole drew attention. In terms of both inhibition constant and isoenzyme selectivity compounds 4-(3-(hydrazinecarbonyl)-5-(4-nitrophenyl)-*1H*-pyrazol-1-yl)benzenesulfonamide (9) for 1,5-diarylpyrazole regioisomer and 4-(4-(hydrazinecarbonyl)-3-(p-tolyl)-*1H*-pyrazol-1-yl)benzenesulfonamide (6b) for 1,3-diarylpyrazole regioisomer can be considered as lead compounds to design novel and more selective compounds towards tumor-related hCA IX isoenzyme for further carbonic anhydrase inhibitors research and development studies.

Table 5
Carbonic anhydrase activity of the 1,3-diarylpyrazole derivatives towards hCA I, hCAII, and hCA IX isoenzymes [26].

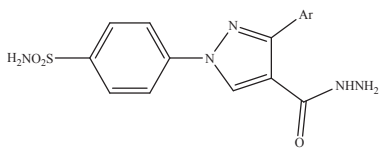

Compound	Ar	Ki (nM)			Selectivity	
		hCA I	hCA II	hCA IX	I/IX	II/IX
6a	Phenyl	7.9	9.3	2.8	2.82	3.32
6b	4-Methylphenyl	9.6	9.2	2.0	4.8	4.6
6g	4-Nitro	32	71	49.3	0.65	1.44
AZA		250	12.1	25	10	0.5

It can also be expressed here, converting ethyl ester derivatives into hydrazide was found a useful modification in increasing hCA IX inhibiting ability of the compounds. This may result different pharmacokinetic and intraction of the compound with targeted enzyme/reseptors than previously reported compounds. For the future perspective, novel pyrazole type compounds can be designed with the hope to find more potent and selective inhibitor by changing substituent on the 3rd position of the ring by the reaction of −COOH or $-CONHNH_2$ groups with other functional groups. For instance, several pyrazole carboxamide derivatives can be synthesized with primary amine derivatives such as amino acids to see the effects of the amide bond on CA inhibitory potency because recently some peptide derivatives were reported as promising CAIs [20].

2.3. Cytotoxicity

1,3,5-Trisubstituted pyrazoles were screened for their *in vitro* cytotoxicities against human oral squamous cell carcinoma (OSCC) cell lines (HSC-2) and human mesenchymal normal oral cells (human gingival fibroblast, HGF) *via* 3-(4,5-Dimethylthiazol-2-yl)-2,5-Diphenyltetrazolium Bromide (MTT) cytotoxicity method according to literature [5,43–53]. Doxorubicine (DXR), 5-Fluorouracil (5-FU) and Methotrexate (MTX) which are anticancer drugs in clinical use for several cancer types were used as reference compounds in the assay. Dose-response of growth inhibition induced by 1,3,5-trisubstituted pyrazoles and references compounds are shown in Fig. 4. Compounds 2, 5 and 11, and DXR showed potent cytotoxicity, killing most of the HSC-2 cells at higher concentration. On the other hand, compounds 3, 6, 8, 9, 12, 5-FU and MTX showed rather cytostatic effects. This may explain that 5-FU and MTX are not used alone, but rather in combination with other anticancer drugs clinically. The results in Table 6 reveal that 50% cytotoxic concentration (CC_{50}) values of the compounds tested were in the range of 37.7– > 200 μM towards HSC-2 malign cell lines while the compounds have cytotoxicities between 132 and > 200 μM against to non-malignant HGF cells. Many compounds tested were found more cytotoxic towards malign cell line than reference drugs 5-FU and MTX, except DXR. Compound ethyl 1-(4-sulfamoylphenyl)-5-(p-tolyl)-*1H*-pyrazole-3-carboxylate, 5 (CC_{50} = 37.7 μM) were found 26.6 and 10.6 times more cytotoxic than reference 5-FU and MTX, respectively. And, compound ethyl 1-(4-sulfamoylphenyl)-5-(thiophen-2-yl)-*1H*-pyrazole-3-carboxylate, 11 (CC_{50} = 58.1 μM) were also found 17.2 and 6.9 times more cytotoxic than 5-FU and MTX, respectively.

Cytotoxicity of tested compounds is desirable when it is more selective towards cancer cells than normal cells. To clarify tumor selectivity potency of the compounds, tumor selectivity (TS) values were calculated by dividing the CC_{50} value towards normal cells into the CC_{50} value towards cancer cell lines (Column B/Column A, Table 6). With regard to this type calculation, compounds 5 (TS = 3.5) and 11 (TS = 2.3) drew attention with the highest TS values among others when compared with reference drugs 5-FU and MTX. This was reflected by wider safety margin of 5 and 11 (indicated by red bidirectional arrow in Fig. 4). Additionally, potency-selectivity expression (PSE) values were calculated according to equation i.e. $(B/A^2) \times 100$ in Table 6 in an attempt to identify the most promising compounds with

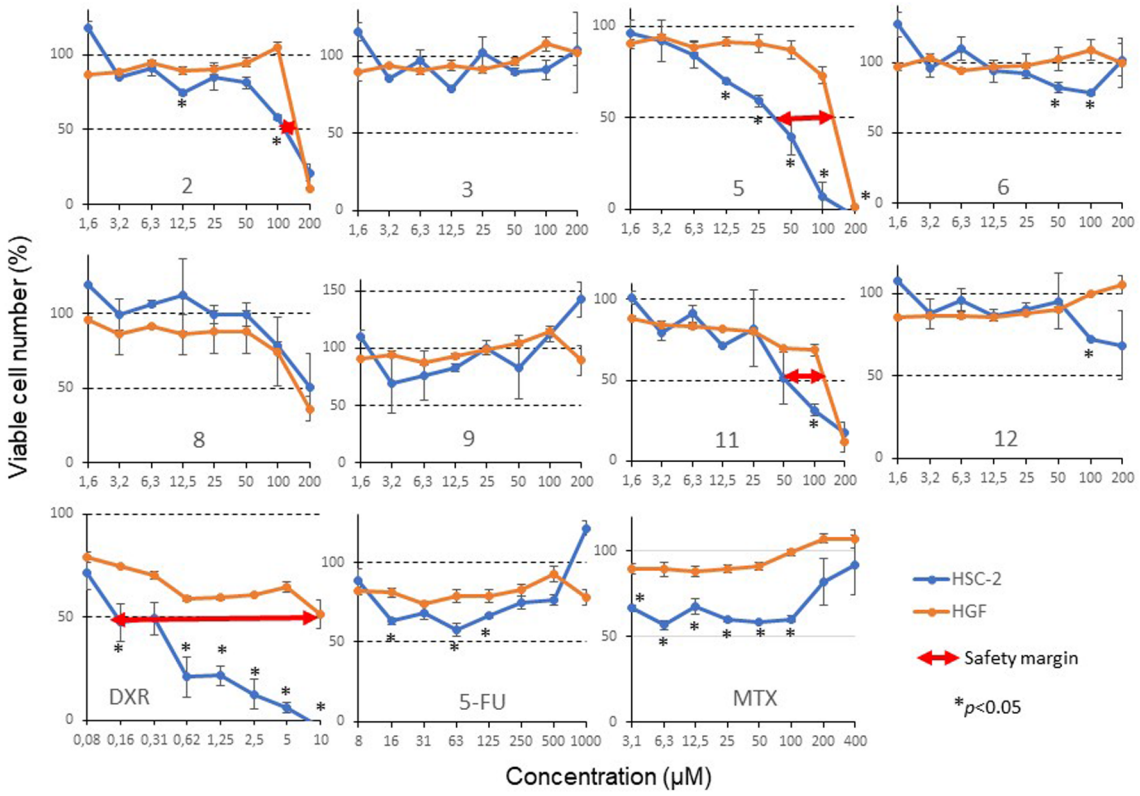

Fig. 4. Dose-response curves of growth inhibition by 1,3,5-trisubstituted pyrazoles and reference compounds against HSC-2 and HGF cells.

Table 6
Anticancer/cytotoxicity results of the compounds 1,3,5-trisubstituted pyrazoles carrying benzenesulfonamide towards HSC-2 and HGF cells.

	CC_{50} (μM)					
	Malignant		Non-malignant			
	HSC-2 (A)	SD	HGF (B)	SD	TS (B/A)	PSE $(B/A^2) \times 100$
2	121.3	6.5	158.3	1.2	1.3	1.1
3	> 200	0.0	> 158	72.5	> < 0.8	> < 0.4
5	37.7	7.2	132.0	4.6	3.5	9.3
6	> 200	0.0	> 200	0.0	> < 1	> < 0.5
8	> 200	0.0	152.2	49.9	< 0.8	> 0.4
9	> 200	0.0	> 200	0.0	> < 1	> < 0.5
11	58.1	19.8	133.0	5.3	2.3	3.9
12	> 199	2.3	> 200	0.0	> < 1	> < 0.5
DXR	0.2	0.2	> 9.6	0.7	> 43.0	> 19229.7
5-FU	> 1000	0.0	> 1000	0.0	> < 1	> < 0.1
MTX	> 400	0.0	> 400	0.0	> < 1	> < 0.25

Each value represents mean from triplicate assays. SD: Standard deviation. TS: Tumor selectivity. PSE: Potency Selectivity Expression. Doxorubicin (DXR), 5-Fluorouracil (5-FU) and Methotrexate (MTX) are reference drugs.

regard to both good potencies and selectively cytotoxic as described in literature [46,52]. Compounds 5 (PSE = 9.3) and 11 (PSE = 3.9) were determined as lead compounds of cytotoxicity assay based on the PSE values.

According to cytotoxicity data, it can be observed that compounds 5 and 11 which are ethyl 1-(4-sulfamoylphenyl)-5-(aryl)-*1H*-pyrazole-3-carboxylate derivatives can be considered for further cytotoxicity studies for detailed results. Hereby, the cytotoxicities of the compounds tested can be affected by several factors such as chemical structures of the compounds, physicochemical properties of the compounds which direct their pharmacological, pharmacokinetics and pharmacodynamics properties of the compounds in tissues. In addition, the method used in cytotoxicity assay, nature of the cell lines used, and mechanism of action of the compounds tested can modify the cytotoxicity results.

It is also necessary to test keratinocyte toxicity of newly manufacturing compounds, since DXR, which showed the broadest safety margin (Fig. 4), killed the normal keratinocyte at micromolar concentration by inducing apoptosis [50].

Oral squamous cell carcinoma (OSCC) is the major malignant tumors of the oral cancers [54]. Despite of improvements in treatment of cancer, the mortality rate for the cancer is still high. Therefore, new prognostic molecular parameters/biomarkers are also needed to enable an individual therapy concept. One of the biomarkers is also reported as CA IX isoenzymes in OSCC patients [13,55,56] while the potential role of another tumor related CA XII as a biomarker in OSCC has not been investigated in detail [57].

Several studies revealed a significant correlation between CAIX expression and clinical stage in OSCC [58]. In accordance with the some cell experiments, the overexpression of CAIX is also associated with increased cell invasive and metastatic ability [59,60]. Therefore, it could be considered that CAIX is an indicator of metastasis in OSCC. Recently, Chien et al. [57], has reported some results in regard to expression of CA XII in a large collection of OSCC tissue samples. In that study, expression of CA XII was detected patients with OSCC and CA XII expression was present in 185/264 patients (70%) cases. According to the results, the expression of CA XII in OSCC samples can predict the progression of OSCC and survival of OSCC patients [57].

When CA inhibitory and cytotoxicites of the compounds compared, the results showed that hydrazide derivative compounds 9 and 12 made attraction in terms of selectively inhibition of cancer related CA IX isoenzyme. On the other hand, surprisingly ester derivatives 5 and 11 showed cytotoxic effects on OSCC lines while compounds 9 and 12 have not shown remarkably cytotoxicity on the same cell lines. Thus, there is a noncompatible situation between CA IX inhibitory potency and inhibition of cell growth of the compounds. It appears possible that the

compounds tested have different mechanism of action on cancer cells except CA IX inhibition. Indeed, the presence of CA IX is not required for killing cancer cells. But, this problematic situation can be clarified by Western Blot analysis in further studies. Additionally, under experimental conditions it is also potential that the compounds undergo chemical inactivation by several chemical reactions and result in blocking the inhibition of the enzyme targeted, and evaluating these uncontrolled situations is also difficult in the context of the experimental media. Additionally, sulfonamide derivatives have also different targets to show its anticancer ability except CA IX isoenzyme. As mentioned above, CA XII is an another cancer related biomarker in OSCC lines. This enzyme can be considered as the new target for the compounds reported here for further studies. In conclusion, to clarify how the compounds showed their bioactivities in different ways, further investigations can be carried out with the next studies.

2.4. *In silico modelling*

Computational modelling, especially computer aided drug design approaches provide powerful tools that enlighten potential inhibition mechanism and help to design more potent drug candidates [61,62]. Although much complicated, isoform selectivity profiles of the studied ligands could also be investigated with the help of *in silico* modelling [18,63,64].

In an attempt to explore selectivity profiles for hCA IX versus hCA I and II, we performed *in silico* modelling of those three structures. Amongst all the compounds, compound 9 exhibits a clear selectivity against hCA IX over hCA II and especially hCA I (Table 4). Subsequent to the molecular docking of compound 9, the binding sites of hCA I, II and IX were aligned. After a detailed visual inspection, a number of amino acid residues were observed to be critical in selectivity (Fig. 5).

Interestingly, compound 9 was observed to have an unusual conformation. The sulfonamide moiety orients itself towards the active site gate. Compound 9 has a large size and hence, a steric hindrance in the binding pocket would show a weaker inhibitory power. At the entrance of the active site, hCA IX has valine (VAL131) that has a small hydrophobic side chain, which results in favourable binding and selectivity towards this isoform. Although there is phenylalanine (PHE131) at this position in hCA II, a plausible π-π interaction with compound 9 is observed. This seems to overcome the diminishing effect of steric clash in the activity.

The amino acid GLN67 in hCA IX has a longer side chain compared with ASN67 of hCA II that could account a slight increase in activity of compound 9 towards hCA IX. The same residue is replaced with a larger amino acid, HIS67 in hCA I which is believed to prevent compound 9 to orient itself in the active conformation. Threonine 200 in the deep active pocket is replaced with histidine 200. Besides being a bulkier substituent, the interaction of imidazole ring in histidine with the benzene ring of compound 9 results in conformational changes.

In addition, the hydrophobic valine (VAL62) located close to the entrance of the active site in hCA I is replaced by a polar asparagine (ASN62) in both hCA II and hCA IX. This polar and bulkier residue causes a steric hindrance and but it also interacts with the polar ends of propeller shaped compound 9 that induces conformational changes enhancing binding and inhibition.

3. Conclusion

In the present paper, 1,3,5-trisubstituted pyrazole benzenesulfonamides were evaluated against physiologically abundant cytosolic hCA I

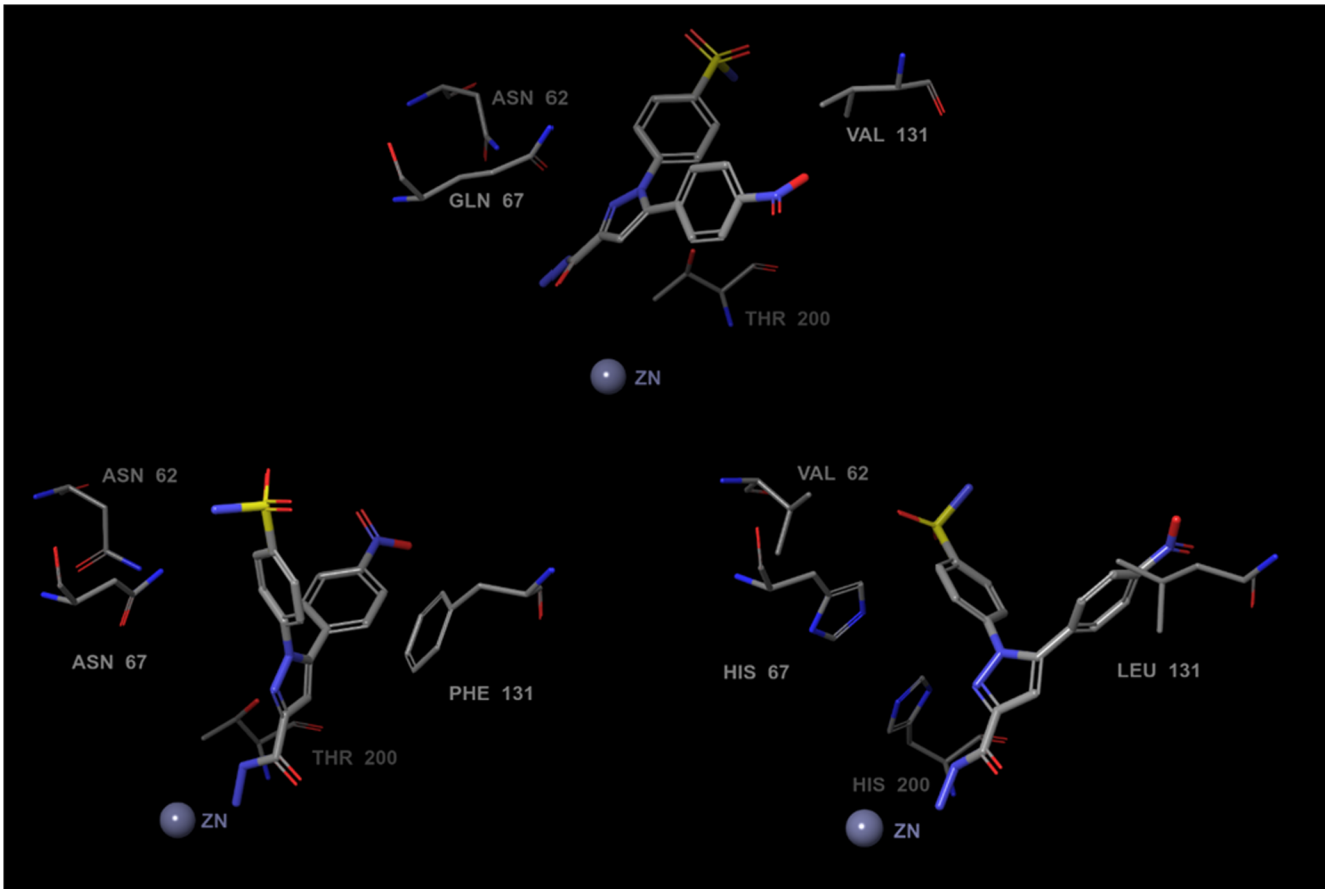

Fig. 5. The binding conformation of compound 9 in the active pocket of hCA IX (top), hCA II (lower left) and hCA I (lower right). Only the discussed critical amino acid residues are shown.

and hCA II and trans-membrane, tumor-associated hCA IX isoforms in terms of carbonic anhydrase inhibition potential and their cytotoxicities were tested against OSCC cell lines. The influence of the substitution pattern at the 5th position of 1,3,5-trisubstituted pyrazole with several aryl groups was examined in terms of their effects on bioactivity. Compounds 6, 8, 9, 11 and 12 showed low nanomolar hCA II inhibitory potency with Ki < 10 nM while compounds 9 and 12 displayed Ki < 10 nM against hCA IX isoenzyme. Compound 9;4-(3-(hydrazinecarbonyl)-5-(4-nitrophenyl)-1*H*-pyrazol-1-yl)benzenesulfonamide, can be considered as the most selective tumor-associated hCA IX inhibitor over off-target cytosolic isoenzymes hCA I and hCA II with the lowest Ki = 2.3 nM values. In addition, its selectivity ratios were 3217 (hCA I/hCA IX) and 3.9 (hCA II/hCA IX). It observed that converting ethyl ester group into the hydrazide group generally enhanced the inhibitory activity of the compounds against hCA IX isoenzyme. Moreover, nature of the substituents present on the 5th position of pyrazole scaffold such as electron-withdrawing nitro group on phenyl ring and bioisosteric replacement of phenyl ring by thiophene affected positively CA inhibitory potency for the 1,5-diaryl pyrazole benzenesulfonamide type compounds. On the other hand, cytotoxicity results pointed out that compounds 5 (CC_{50} = 37.7 μM) and 11 (CC_{50} = 58.1 μM) can be considered as lead compounds of the cytotoxicity study since they were more cytotoxic than reference drugs 5-FU and MTX. The results obtained from *in silico* modelling showed that specific residues within the binding pocket of hCA I, II and IX might provide the rationale for selective inhibition of hCA IX over I and II. In the light of the bioactivity results of this current study, using of 4-(3-(hydrazinecarbonyl)-5-aryl-1*H*-pyrazol-1-yl)benzenesulfonamide scaffold and its derivatives could provide a rational approach because of their promising selectivity and inhibitory potency against cancer-related hCA IX isoenzyme as anticancer drug candidates for research and development studies of CAIs.

4. Material and methods

4.1. Chemistry

Reagents and solvents were purchased from commercial sources and used without further purification. Nuclear Magnetic Resonance (NMR) spectra (^{1}H NMR) and Nuclear Overhauser Spectroscopy (NOESY) spectra of the compounds were recorded with 400 MHz Varian (Danbury, ABD) spectrometer. Chemical shifts (δ) were reported in ppm. $CDCl_3$ (Merck) and DMSO-d_6 (Merck) were used as NMR solvent. High-Resolution Mass Spectra (HRMS) of the compounds were taken using a liquid chromatography ion trap-time of the flight tandem mass spectrometer (Shimadzu, Kyoto, Japan) equipped with an electrospray ionization (ESI) source, operating in both positive and negative ionization mode. Shimadzu's LCMS Solution software was used for data analysis. Melting points were determined using an Electrothermal 9100 instrument (IA9100, Bibby Scientific Limited, Staffordshire, UK) and are uncorrected. Process of the reaction was monitored by Thin Layer Chromatography (TLC) using Silicagel HF254 (Merck Art 5715) plate under UV lamb (254 and 365 nm, Spectroline, Model ENF-240C/FE, Spectronics Corporation Westbury, New York U.S.A).

Synthesis of the ethyl 2,4-dioxo-4-phenylbutanoate (1) and ethyl 2,4-dioxo-4-(p-tolyl)butanoate (4, Scheme 1**)** [40,65–69]

Diethyl oxalate (140 mmol for 1; 120 mmol for 4) and acetophenone (140 mmol for 1; 120 mmol for 4) was respectively added into the freshly prepared sodium ethoxide [(100 ml ethanol and 140 mmol sodium for 1); (100 ml ethanol and 120 mmol sodium for 2)] on ice bath. Then additional 200 ml ethanol was added into the yellow color mixture and the final mixture was stirred at room temperature. The reaction process was monitored by TLC using ethylacetate: hexane (2:3) solvent system. After the reaction was stopped (20 h for 1; 30 h for 4), distilled water (50 ml) was added into the reaction mixture and then pH was adjusted to pH = 3 by adding hydrochloride acid (37%) dropwise. The aqueous mixture was extracted with ethylacetate (3 × 25 ml). The combined extracts were dried on dry $MgSO_4$, and the content of the mixture was concentrated under vacuum and then kept at room temperature to obtain the final product. The compounds solidified were filtered, washed with cold ethanol and then dried at room temperature. Physical and spectral data of the compounds were given as below.

Ethyl 2,4-dioxo-4-phenylbutanoate, 1: Light orange solid, yield 50%. Mp = 38–40 °C. ^{1}H NMR ($CDCl_3$, 400 MHz, δ, ppm): 15.30 (bs, 1H, OH), 7.98–7.96 (m, 2H, ArH), 7.60–7.53 (m, 1H, ArH), 7.49–7.46 (m, 2H, ArH), 7.05 (s, 1H, −COCH═C−), 4.37 (q, J = 7.1 Hz, 2H, $-OCH_2CH_3$), 1.39 (t, J = 7.1 Hz, 3H, $-OCH_2CH_3$). HRMS (ESI-MS) *m/z* Calculated: 221.0808 $C_{12}H_{13}O_4$ $[M+H]^+$; Found: 221.0797.

Ethyl 2,4-dioxo-4-(p-tolyl)butanoate, 4: Light orange solid, yield 54%. Mp = 109–111 °C. ^{1}H NMR ($CDCl_3$, 400 MHz, δ, ppm): 14.80 (bs, 1H, −OH), 7.89 (d, J = 8.2 Hz, 2H, ArH), 7.29 (d, J = 8.2 Hz, 2H, ArH), 7.05 (s, 1H, −COCH═C−), 4.39 (q, J = 7.1 Hz, 2H, $-OCH_2CH_3$), 2.43 (s, 3H, $ArCH_3$), 1.40 (t, J = 7.1 Hz, 3H, $-OCH_2CH_3$). HRMS (ESI-MS) *m/z* Calculated: 257.0784 $C_{13}H_{14}O_4$ $[M+Na]^+$; Found: 257.0778.

Synthesis of the ethyl 4-(4-nitrophenyl)-2,4-dioxobutanoate (7, Scheme 1**)** [40,65–69]

Sodium ethoxide (182 mmol) was stirred in ethanol (200 ml) on an ice bath, after 10 min, diethyl oxalate (91 mmol) was added into the orange color mixture. Then, 4-nitro acetophenone (91 mmol) was added slowly into the previous mixture and the color of the main mixture turned into dark brown. The reaction process was monitored by TLC using dichloromethane: methanol (4.8:0.2) solvent system. After 20 h, distilled water (100 ml) was added into the reaction mixture and then pH was adjusted to pH = 2–3 by adding hydrochloride acid (37%) dropwise. The aqueous mixture was extracted with ethylacetate (3 × 50 ml). The combined extracts were dried on dry Na_2SO_4, and the content of the mixture was concentrated under vacuum and then kept at room temperature to obtain a crude product. It was crystallized from ethanol. Ethyl 4-(4-nitrophenyl)-2,4-dioxobutanoate, 7: Light brown solid, yield 20%. Mp = 111–113 °C. ^{1}H NMR ($CDCl_3$, 400 MHz, δ, ppm): 8.34 (d, J = 8.8 Hz, 2H, ArH), 8.14 (d, J = 8.8 Hz, 2H, ArH), 7.09 (s, 1H, −COCH═C−), 4.34 (q, J = 7.1 Hz, 2H, $-OCH_2CH_3$), 1.42 (t, J = 7.1 Hz, 3H, $-OCH_2CH_3$). HRMS (ESI-MS) *m/z* Calculated: 266.0659 $C_{12}H_{12}NO_6$ $[M+H]^+$; Found: 266.0665.

Synthesis of ethyl 2,4-dioxo-4-(thiophen-2-yl)butanoate (10, Scheme 1**)** [40,65–69]

2-Acetylthiophen (159 mmol) and diethyl oxalate (318 mmol) was stirred in THF (250 ml) at rt for 10 min. Then, sodium ethoxide (318 mmol) was added slowly onto the colorless mixture. The reaction process was monitored by TLC using ethylacetate: hexane (3:2) solvent system. After 6 h, the content of the reaction was poured into hexane (250) and the mixture was stirred at room temperature for 15 min. Then, 1N HCl aqueous solution (250 ml) was added into the mixture and stirred for 30 min at room temperature. The light brown solid obtained was washed with water then dried. Ethyl 2,4-dioxo-4-(thiophen-2-yl)butanoate, 10: Light brown solid, yield 50%. Mp = 40–42 °C. ^{1}H NMR ($CDCl_3$, 400 MHz, δ, ppm): 7.84 (dd, J = 4.0, 1.1 Hz, 1H, ArH), 7.74 (dd, J = 5.0, 1.1 Hz, 1H, ArH), 7.18 (dd, J = 5.0, 4.0 Hz, 1H, ArH), 6.91 (s, 1H, −COCH═C−), 4.38 (q, J = 7.2 Hz, 2H, $-OCH_2CH_3$), 1.40 (t, J = 7.2 Hz, 3H, $-OCH_2CH_3$). HRMS (ESI-MS) *m/z* Calculated: 249.0192 $C_{10}H_{11}O_4S$ $[M+Na]^+$; Found: 249.0180.

Synthesis of ethyl 5-aryl-1-(4-sulfamoylphenyl)-*1H*-pyrazole-3-carboxylate derivatives (2, 5, 8, 11, Scheme 1**)** [40,65–69]

A suitable diketoester, ethyl 2,4-dioxo-4-phenylbutanoate (1) and

ethyl 2,4-dioxo-4-(p-tolyl)butanoate (4), ethyl 4-(4-nitrophenyl)-2,4-dioxobutanoate (7), ethyl 2,4-dioxo-4-(thiophen-2-yl)butanoate (10) were used as a starting material with the aim to synthesize compounds 2, 5, 8, and 11, respectively.

A suitable starting compound [1 (22 mmol), 4 (21.3 mmol), 7 (19 mmol), 10 (65 mmol)] was dissolved in a suitable amount ethanol (50 ml for 1, 100 ml for 4, 200 ml for 7, 150 ml for 10) by heating and then 4-hydrazinobenzenesulfonamide hydrochloride (22 mmol for 1, 21.3 mmol for 4, 19 mmol for 7, 65 mmol for 10) was added onto the mixture. The reaction process was monitored by TLC using dichloromethane: methanol (4.8:0.2) solvent system. The orange color reaction mixture was refluxed for several hours as 6 h for 1, 7 h for 4, 6 h for 7, 3 h for 10. The content of the reaction mixture was concentrated half of its volume under vacuum and then kept at room temperature. The formed precipitate was filtered, dried and crystallized from ethanol. All spectral data confirmed the chemical structure of the compounds.

Ethyl 5-phenyl-1-(4-sulfamoylphenyl)-*1H*-pyrazole-3-carboxylate, 2: White color solid. Yield 71%. Mp = 192–195 °C, 192–194 °C [70]. ^{1}H NMR (DMSO-d_6, 400 MHz, δ, ppm): 7.84 (d, J = 8.4 Hz, 2H, ArH), 7.51–7.44 (m, 4H, ArH, -SO_2NH_2), 7.39–7.34 (m, 3H, ArH), 7.29–7.27 (m, 2H, ArH), 7.14 (s, 1H, H-4 pyrazole), 4.32 (q, J = 7.1 Hz, 2H, $-OCH_2CH_3$), 1.30 (t, J = 7.1 Hz, 3H, $-OCH_2CH_3$). HRMS (ESI-MS) m/z Calculated: 372.1013 $C_{18}H_{18}N_3O_4S$ $[M+H]^+$; Found: 372.1001.

Ethyl 1-(4-sulfamoylphenyl)-5-(p-tolyl)-*1H*-pyrazole-3-carboxylate, 5: Cream color solid, yield 91%. Mp = 227–229 °C, 224–226 °C [40]. ^{1}H NMR (DMSO-d_6, 400 MHz, δ, ppm): 7.85 (d, J = 8.8 Hz, 2H, ArH), 7.51–7.49 (m, 4H, ArH, $-SO_2NH_2$), 7.20–7.14 (m, 4H, ArH), 7.08 (s, 1H, H-4 pyrazole), 4.31 (q, J = 7.0 Hz, 2H, $-OCH_2CH_3$), 2.29 (s, 3H, $ArCH_3$), 1.30 (t, J = 7.0 Hz, 3H, $-OCH_2CH_3$). HRMS (ESI-MS) m/z Calculated: 386.1169 $C_{19}H_{20}N_3O_4S$ $[M+H]^+$; Found: 386.1161.

Ethyl 5-(4-nitrophenyl)-1-(4-sulfamoylphenyl)-*1H*-pyrazole-3-carboxylate, 8: Cream color solid, yield 89%. Mp = 194–196 °C. ^{1}H NMR (DMSO-d_6, 400 MHz, δ, ppm): 8.22 (d, J = 8.8 Hz, 2H, ArH), 7.86 (d, J = 8.4 Hz, 2H, ArH), 7.58–7.54 (m, 4H, ArH), 7.51 (s, 2H, $-SO_2NH_2$), 7.35 (s, 1H, H-4 pyrazole), 4.34 (q, J = 7.1 Hz, 2H, $-OCH_2CH_3$), 1.31 (t, J = 7.1 Hz, 3H, $-OCH_2CH_3$). HRMS (ESI-MS) m/z Calculated: 417.0863 $C_{18}H_{17}N_4O_6S$ $[M+H]^+$; Found: 417.0846.

Ethyl 1-(4-sulfamoylphenyl)-5-(thiophen-2-yl)-*1H*-pyrazole-3-carboxylate, 11: Cream solid, yield 80%. Mp = 198–200 °C, 197–199 °C [69]. ^{1}H NMR (DMSO-d_6, 400 MHz, δ, ppm): 7.92 (d, J = 8.8 Hz, 2H, ArH), 7.67–7.64 (m, 3H, ArH), 7.56 (s, 2H, $-SO_2NH_2$), 7.17 (s, 1H, H-4 pyrazole), 7.16 (dd, J = 3.7, 2.6 Hz, 1H, ArH), 7.08 (dd, J = 5.1, 3.7 Hz, 1H, ArH), 4.32 (q, J = 7.0 Hz, 2H, $-OCH_2CH_3$), 1.29 (t, J = 7.0 Hz, 3H, $-OCH_2CH_3$). HRMS (ESI-MS) m/z Calculated: 378.0577 $C_{16}H_{16}N_3O_4S_2$ $[M+H]^+$; Found: 378.0561.

Synthesis of 4-(3-(hydrazinecarbonyl)-5-aryl-*1H*-pyrazol-1-yl) benzenesulfonamide derivatives (3, 6, 9, 12, Scheme 1**) [40,65–69]**

A suitable pyrazole-3-carboxylate derivatives, ethyl 5-phenyl-1-(4-sulfamoylphenyl)-*1H*-pyrazole-3-carboxylate (2), ethyl 1-(4-sulfamoylphenyl)-5-(p-tolyl)-*1H*-pyrazole-3-carboxylate (5), ethyl 5-(4-nitrophenyl)-1-(4-sulfamoylphenyl)-*1H*-pyrazole-3-carboxylate (8), ethyl 1-(4-sulfamoylphenyl)-5-(thiophen-2-yl)-*1H*-pyrazole-3-carboxylate (11) were used as a starting material to synthesize 3, 6, 9, and 12, respectively.

An appropriate pyrazole-3-carboxylate derivative [2 (16 mmol), 5 (18 mmol), 8 (14 mmol), 11 (27 mmol)] was dissolved in ethanol (100 ml for 2 and 5) and methanol (200 ml for 8 and 11) by heating. Afterwards, the reaction mixture was refluxed after adding hydrazine hydrate (99%) (320 mmol for 2, 360 mmol for 5, 280 mmol for 8 and 540 mmol for 12). The reaction process was monitored by TLC using dichloromethane:metanol (4.8:0.2) solvent system. After 4–25 h, the reaction content was poured into the ice-water (100 ml for 3 and 9, 50 ml for 6, 150 ml for 12). Glacial acetic acid (2–4 ml) was added into the mixture and then stirred at room temparature until whitish precipitate formed. The solid obtained was filtered, washed with water and alcohol, then dried and crystallized from ethanol to obtain pure compounds as 3, 6, 9, and 12.

4-(3-(Hydrazinecarbonyl)-5-phenyl-*1H*-pyrazol-1-yl)benzenesulfonamide, 3: White solid, yield 90%. Mp = 265–267 °C, 265 °C [68]. ^{1}H NMR (DMSO-d_6, 400 MHz, δ, ppm): 9.61 (s, 1H, −CONH−), 7.83 (d, J = 8.8 Hz, 2H, ArH), 7.49 (d, J = 8.4 Hz, 2H, ArH), 7.40–7.38 (m, 5H, ArH), 7.28–7.26 (m, 2H, ArH), 7.01 (s, 1H, H-4 pyrazole), 4.48 (s, 2H, $-NHNH_2$). HRMS (ESI-MS) m/z Calculated: 358.0968 $C_{16}H_{16}N_5O_3S$ $[M+H]^+$; Found: 358.0954.

4-(3-(Hydrazinecarbonyl)-5-(p-tolyl)-*1H*-pyrazol-1-yl)benzenesulfonamide, 6: White solid, yield 51%. Mp = 193–195 °C. ^{1}H NMR (DMSO-d_6, 400 MHz, δ, ppm): 9.59 (s, 1H, −CONH−), 7.82 (d, J = 8.4 Hz, 2H, ArH), 7.51–7.47 (m, 4H, ArH, $-SO_2NH_2$), 7.19 (d, J = 8.4 Hz, 2H, ArH), 7.14 (d, J = 8.1 Hz, 2H, ArH), 6.97 (s, 1H, H-4 pyrazole), 4.48 (s, 2H, $-NHNH_2$), 2.29 (s, 3H, $ArCH_3$). HRMS (ESI-MS) m/z Calculated: 372.1125 $C_{17}H_{18}N_5O_3S$ $[M+H]^+$; Found: 372.1114.

4-(3-(Hydrazinecarbonyl)-5-(4-nitrophenyl)-*1H*-pyrazol-1-yl)benzenesulfonamide, 9: Cream solid, yield % 81. Mp = 305–307 °C. ^{1}H NMR (DMSO-d_6, 400 MHz, δ, ppm): 9.68 (s, 1H, −CONH−), 8.22 (d, J = 8.8 Hz, 2H, ArH), 7.85 (d, J = 8.8 Hz, 2H, ArH), 7.84–7.52 (m, 6H, ArH, $-SO_2NH_2$), 7.21 (s, 1H, H-4 pyrazole). HRMS (ESI-MS) m/z Calculated: 403.0819 $C_{16}H_{15}N_6O_5S$ $[M+H]^+$; Found: 403.0812.

4-(3-(Hydrazinecarbonyl)-5-(thiophen-2-yl)-*1H*-pyrazol-1-yl)benzenesulfonamide, 12: White solid, yield 86%. Mp = 210–212 °C. ^{1}H NMR (DMSO-d_6, 400 MHz, δ, ppm): 10.2 (s, 1H, −CONH−), 7.93 (d, J = 8.8 Hz, 2H, ArH), 7.68–7.65 (m, 3H, ArH), 7.54 (s, 2H, $-SO_2NH_2$), 7.19 (s, 1H, H-4 pyrazole), 7.15 (d, J = 3.3 Hz, 1H, ArH), 7.10–7.07 (m, 1H, ArH). HRMS (ESI-MS) m/z Hesaplanan: 364.0533 $C_{14}H_{14}N_5O_3S_2$ $[M+H]^+$; Found: 364.0523.

4.2. Crystallography

For the crystal structure determination, single-crystal of compound 2 was used for the data collection on a four-circle Rigaku R-AXIS RAPID-S diffractometer (equipped with a two-dimensional area IP detector). Graphite-monochromated Mo-K_α radiation (λ = 0.71073 Å) and oscillation scans technique with $\Delta w = 5^\circ$ for one image were used for data collection. The lattice parameters were determined by the least-squares methods based on all reflections with $F^2 > 2\sigma(F^2)$. Integration of the intensities, correction for Lorentz and polarization effects and cell refinement were performed using CrystalClear (Rigaku/MSC Inc., 2005) software (Rigaku/MSC, Inc., 9009 New Trails Drive, TheWoodlands, TX 7738.) The structure was solved by direct methods using SHELXS-97 [71] and non-hydrogen atoms were refined using anisotropic displacement parameters by a full-matrix least-squares procedure using the program SHELXL-97. H atoms were positioned geometrically and refined using a riding model. The final difference Fourier maps showed no peaks of chemical significance. Crystal data for compound 2*:* $C_{18}H_{17}N_3O_4S$, crystal system, space group: monoclinic, $P2_1/c$; (no:14); unit cell dimensions: a = 7.9535(7), b = 16.5706(17), c = 14.0579(14) Å, α = 90, β = 93.939(3), γ = 90°; volume; 1848.4(3) Å^3, Z = 4; calculated density: 1.33 g/cm^3; absorption coefficient: 0.203 mm^{-1}; F(0 0 0): 766; θ-range for data collection 2.8–26.4°; refinement method: full matrix least-square on F^2; data/parameters: 2924/236; goodness-of-fit on F^2: 1.184; final R-indices [$I > 2\sigma(I)$]: R_1 = 0.075, wR_2 = 0.20; largest diff. peak and hole: 0.780 and −0.707 e Å^{-3}.

Crystallographic data that were deposited in CSD under CCDC-1912930 registration number contains the supplementary crystallographic data for this structure (compound 2). These data can be obtained free of charge from the Cambridge Crystallographic Data Centre (CCDC) via www.ccdc.cam.ac.uk/data_request/cif and are available free of charge upon request to CCDC, 12 Union Road, Cambridge, UK

(fax: +441223 336033, e-mail: deposit@ccdc.cam.ac.uk).

4.3. Computational part

High-resolution protein crystal structures of human CAI (PDB ID: 4LXZ, 1.55 Å), CAII (PDB ID: 3HS4, 1.1 Å) and CAIX (PDB ID: 3IAI, 2.2 Å) in complexed with a native ligand were downloaded from RCSB Protein Data Bank and prepared using Schrödinger's [72] Protein Preparation Wizard [73,74]. Charges and bond orders were assigned, hydrogens were added to the heavy atoms, chain A, native ligands and Zinc metal were kept. All water molecules and heteroatoms were removed and the final structure were optimised. Finally, in order to avoid steric clashes between the atoms, minimisation was performed until heavy atoms were converged to a RMSD of 0.3 Å.

The studied ligands were also prepared by subjecting to LigPrep [75] tool in the Schrödinger software. The 3D structures including all possible low energy ionisation and tautomeric states within the pH range of 7.0 ± 2 were generated and then geometrically minimised.

The binding site of hCA isoforms were defined by generating a grid around the native ligand. The default setting for the grid size was changed to allow ligands having ≤20 Å size to be docked. Glide XP (extra precision) [76,77] module was used to dock the compounds into the active site. The default OPLS3e7 force field was used throughout all calculations.

4.4. Bioactivity

4.4.1. Carbonic anhydrase inhibition

An SX.18MV-R Applied Photophysics (Oxford, UK) stopped-flow instrument was used to assay the catalytic/inhibition of various CA isoenzymes [42]. Phenol Red (at a concentration of 0.2 mM) has been used as an indicator, working at the absorbance maximum of 557 nm, with 10 mM Hepes (pH 7.4) as a buffer, 0.1 M Na_2SO_4 or $NaClO_4$ (for maintaining constant the ionic strength; these anions are not inhibitory in the used concentration), following the CA-catalyzed CO_2 hydration reaction for a period of 5–10 s. Saturated CO_2 solutions in the water at 25 °C were used as substrate. Stock solutions of inhibitors were prepared at a concentration of 10 mM (in DMSO) and further diluted to appropriate concentrations dilutions with the assay buffer mentioned above. At least 7 different inhibitor concentrations have been used for measuring the inhibition constant. Inhibitor and enzyme solutions were preincubated together for 10 min at room temperature prior to assay, in order to allow for the formation of the E-I complex. Triplicate experiments were done for each inhibitor concentration, and the values reported throughout the paper are the mean of such results. The inhibition constants were obtained by nonlinear least-squares methods using the Cheng-Prusoff equation, as reported earlier and represent the mean from at least three different determinations. All CA isozymes used here were recombinant proteins obtained as reported earlier [4,5,45–47,68,78,79].

4.4.2. Cytotoxic activity

The following chemicals and reagents were obtained from the indicated companies: Dulbecco's modified Eagle's medium (DMEM), from GIBCO BRL, Grand Island, NY, USA; fetal bovine serum (FBS), 3-(4,5-dimethylthiazol-2-yl)-2,5-diphenyltetrazolium bromide (MTT), doxorubicin, dimethyl sulfoxide (DMSO) from Wako Pure Chem. Ind., Osaka, Japan; 5-fluorouracil (5-FU) from Kyowa (Tokyo, Japan); methotrexate from Nacalai Tesque, Inc., Kyoto, Japan; Culture plastic dishes and plates (96-well) were purchased from Becton Dickinson (Franklin Lakes, NJ, USA).

Human normal oral mesenchymal cells (human gingival fibroblast, HGF), established from the first premolar tooth extracted from the lower jaw of a 12-year-old girl [80], and human oral squamous cell carcinoma cell line HSC-2 (derived from tongue) purchased from Riken Cell Bank (Tsukuba, Japan), were cultured at 37 °C in DMEM supplemented with 10% heat-inactivated FBS, 100 units/ml, penicillin G and 100 μg/ml streptomycin sulfate under a humidified 5% CO_2 atmosphere. HGF cells at 10–18 population doubling levels were used in the present study.

Assay for cytotoxic activity. Cells were inoculated at 2.5×10^3 cells/0.1 ml in a 96-microwell plate (Becton Dickinson Labware, Franklin Lakes, NJ, U.S.A.). After 48 h, the medium was replaced with 0.1 ml of fresh medium containing different concentrations of single test compounds. Cells were incubated further for 48 h and the relative viable cell number was then determined by the MTT method [43]. The relative viable cell number was determined by the absorbance of the cell lysate at 562 nm, using a microplate reader (Sunrise Rainbow RC-R; TECAN, Männedorf, Switzerland). Control cells were treated with the same amounts of DMSO and the cell damage induced by DMSO was subtracted from that induced by test agents. The concentration of compound that reduced the viable cell number by 50% (CC_{50}) was determined from the dose-response curve and the mean value of CC_{50} for each cell type was calculated from triplicate assays as described before [5,43–48,51–53,81–84]. Calculation of tumor-selectivity index (TS). TS was calculated using the following equation as TS = CC_{50} against HGF non-malignant cells/CC_{50} against malignant HSC-2 cells [(B/A) in Table 6]. We have confirmed that the TS value thus determined reflects the antitumor potential of test samples, although normal and tumor cells are derived from different tissues (mesenchymal or epithelial tissues, respectively) [85]. We did not use human normal oral keratinocytes as controls, since doxorubicin and 5-fluorouracil showed potent cytotoxicity against these epithelial cells by an as yet unidentified mechanism.

Calculation of potency-selectivity expression (PSE). PSE was calculated using the following equation: PSE = TS/CC_{50} against tumor cells × [that is, (B/A^2) × 100 in Table 6)] [49,52]. Statistical treatment. Experimental data are the mean ± standard deviation (SD). The statistical differences between control and treated groups were evaluated by paired Student's *t*-test. A value of $p < 0.05$ was considered to be significant.

Acknowledgments

Dr. Cem Yamali was financially supported by The Scientific and Technological Research Council of Turkey (TUBITAK), Ankara, Turkey (Grant Number: 2214-A/1059B141601251) with 2214-A International Ph.D. Research Scholarship Program for his Ph.D. thesis in 2018. Authors also thank Dr. Yusuf Ozkay and MSc. Serkan Levent (Anadolu University, Turkey) for HRMS and Ataturk University, Department of Chemistry for NMR results.

Declaration of interest

The authors report no conflict of interest and are responsible for the contents and writing of the paper.

Appendix A. Supplementary material

Supplementary data to this article can be found online at https://doi.org/10.1016/j.bioorg.2019.103222.

References

[1] A. Nocentini, C.T. Supuran, Carbonic anhydrase inhibitors as antitumor/antimetastatic agents: a patent review (2008–2018), Expert Opin. Ther. Pat. 28 (2018) 729–740.
[2] C.T. Supuran, Structure and function of carbonic anhydrases, Biochem. J. 473 (2016) 2023–2032.
[3] C.T. Supuran, Carbonic anhydrase inhibitors and their potential in a range of therapeutic areas, Expert Opin. Ther. Pat. 28 (2018) 709–712.
[4] H.I. Gul, C. Yamali, M. Bulbuller, P.B. Kirmizibayrak, M. Gul, A. Angeli, S. Bua, C.T. Supuran, Anticancer effects of new dibenzenesulfonamides by inducing apoptosis and autophagy pathways and their carbonic anhydrase inhibitory effects

on hCA I, hCA II, hCA IX, hCA XII isoenzymes, Bioorg. Chem. 78 (2018) 290–297.
[5] H.I. Gul, C. Yamali, H. Sakagami, A. Angeli, J. Leitans, A. Kazaks, K. Tars, D.O. Ozgun, C.T. Supuran, New anticancer drug candidates sulfonamides as selective hCA IX or hCA XII inhibitors, Bioorg. Chem. 77 (2018) 411–419.
[6] S.M. Monti, C.T. Supuran, G. De Simone, Anticancer carbonic anhydrase inhibitors: a patent review (2008–2013), Expert Opin. Ther. Pat. 23 (2013) 737–749.
[7] C.T. Supuran, Carbonic anhydrase inhibition and the management of hypoxic tumors, Metabolites 7 (2017) 48–61.
[8] J. Meehan, C. Ward, A. Turnbull, J. Bukowski-Wills, A.J. Finch, E.J. Jarman, C. Xintaropoulou, C. Martinez-Perez, M. Gray, M. Pearson, P. Mullen, C.T. Supuran, F. Carta, D.J. Harrison, I.H. Kunkler, S.P. Langdon, Inhibition of pH regulation as a therapeutic strategy in hypoxic human breast cancer cells, Oncotarget 8 (2017) 42857–42875.
[9] F. Carta, C.T. Supuran, A. Scozzafava, Sulfonamides and their isosters as carbonic anhydrase inhibitors, Future Med. Chem. 6 (2014) 1149–1165.
[10] Y. Lou, P.C. McDonald, A. Oloumi, S. Chia, C. Ostlund, A. Ahmadi, A. Kyle, U. Auf dem Keller, S. Leung, D. Huntsman, B. Clarke, B.W. Sutherland, D. Waterhouse, M. Bally, C. Roskelley, C.M. Overall, A. Minchinton, F. Pacchiano, F. Carta, A. Scozzafava, N. Touisni, J.Y. Winum, C.T. Supuran, S. Dedhar, Targeting tumor hypoxia: suppression of breast tumor growth and metastasis by novel carbonic anhydrase IX inhibitors, Cancer Res. 71 (2011) 3364–3376.
[11] F. Pacchiano, F. Carta, P.C. McDonald, Y. Lou, D. Vullo, A. Scozzafava, S. Dedhar, C.T. Supuran, Ureido-substituted benzenesulfonamides potently inhibit carbonic anhydrase IX and show antimetastatic activity in a model of breast cancer metastasis, J. Med. Chem. 54 (2011) 1896–1902.
[12] P.C. McDonald, J.Y. Winum, C.T. Supuran, S. Dedhar, Recent developments in targeting carbonic anhydrase IX for cancer therapeutics, Oncotarget 3 (2012) 84–97.
[13] J.S. Yang, C.W. Lin, C.Y. Chuang, S.C. Su, S.H. Lin, S.F. Yang, Carbonic anhydrase IX overexpression regulates the migration and progression in oral squamous cell carcinoma, Tumour Biol. 36 (2015) 9517–9524.
[14] E.R. Swenson, Safety of carbonic anhydrase inhibitors, Expert Opin. Drug Saf. 13 (2014) 459–472.
[15] C.T. Supuran, Inhibition of carbonic anhydrase IX as a novel anticancer mechanism, World J. Clin. Oncol. 3 (2012) 98–103.
[16] K. D'Ambrosio, R.M. Vitale, J.M. Dogne, B. Masereel, A. Innocenti, A. Scozzafava, G. De Simone, C.T. Supuran, Carbonic anhydrase inhibitors: bioreductive nitro-containing sulfonamides with selectivity for targeting the tumor associated isoforms IX and XII, J. Med. Chem. 51 (2008) 3230–3237.
[17] N. Chiaramonte, M.N. Romanelli, E. Teodori, C.T. Supuran, Amino acids as building blocks for carbonic anhydrase inhibitors, Metabolites 8 (2018) 36–58.
[18] Z.C. Mam, Y. Mboge, Alyssa Wolff, John V. Mathias, Tu. Chingkuang, Kevin D. Brown, Murat Bozdag, Fabrizio Carta, Claudiu T. Supuran, Robert McKenna, Susan C. FrostID, Selective inhibition of carbonic anhydrase IX over carbonic anhydrase XII in breast cancer cells using benzene sulfonamides: disconnect between activity and growth inhibition, PLoS ONE 13 (2018) 1–27.
[19] C.T. Supuran, How many carbonic anhydrase inhibition mechanisms exist? J. Enzyme Inhib. Med. Chem. 31 (2016) 345–360.
[20] A. Mollica, R. Costante, A. Akdemir, S. Carradori, A. Stefanucci, G. Macedonio, M. Ceruso, C.T. Supuran, Exploring new Probenecid-based carbonic anhydrase inhibitors: synthesis, biological evaluation and docking studies, Bioorg. Med. Chem. 23 (2015) 5311–5318.
[21] F. Carta, D. Vullo, S.M. Osman, Z. AlOthman, C.T. Supuran, Synthesis and carbonic anhydrase inhibition of a series of SLC-0111 analogs, Bioorg. Med. Chem. 25 (2017) 2569–2576.
[22] C.T. Supuran, Carbonic anhydrase inhibitors as emerging agents for the treatment and imaging of hypoxic tumors, Expert Opin. Investig. Drugs. 27 (2018) 963–970.
[23] W.M. Eldehna, M.F. Abo-Ashour, E. Berrino, D. Vullo, H.A. Ghabbour, S.T. Al-Rashood, G.S. Hassan, H.M. Alkahtani, A.A. Almehizia, A. Alharbi, H.A. Abdel-Aziz, C.T. Supuran, SLC-0111 enaminone analogs, 3/4-(3-aryl-3-oxopropenyl) aminobenzenesulfonamides, as novel selective subnanomolar inhibitors of the tumor-associated carbonic anhydrase isoform IX, Bioorg. Chem. 83 (2019) 549–558.
[24] C.T. Supuran, Indisulam: an anticancer sulfonamide in clinical development, Expert Opin. Investig. Drugs 12 (2003) 283–287.
[25] D.C. Talbot, J. von Pawel, E. Cattell, S.M. Yule, C. Johnston, A.S. Zandvliet, A.D. Huitema, C.J. Norbury, P. Ellis, L. Bosquee, M. Reck, A randomized phase II pharmacokinetic and pharmacodynamic study of indisulam as second-line therapy in patients with advanced non-small cell lung cancer, Clin. Cancer Res. 13 (2007) 1816–1822.
[26] P. Khloya, G. Celik, SitaRam, D. Vullo, C.T. Supuran, P.K. Sharma, 4-Functionalized 1,3-diarylpyrazoles bearing benzenesulfonamide moiety as selective potent inhibitors of the tumor associated carbonic anhydrase isoforms IX and XII, Eur. J. Med. Chem. 76 (2014) 284–290.
[27] R. Rajendra, R.L. Jones, S.M. Pollack, Targeted treatment for advanced soft tissue sarcoma: profile of pazopanib, Onco. Targets Ther. 6 (2013) 217–222.
[28] S.T. Kim, H.L. Jang, S.J. Lee, J. Lee, Y.L. Choi, K.M. Kim, J. Cho, S.H. Park, Y.S. Park, H.Y. Lim, M. Yashiro, W.K. Kang, J.O. Park, Pazopanib, a novel multitargeted kinase inhibitor, shows potent in vitro antitumor activity in gastric cancer cell lines with FGFR2 amplification, Mol. Cancer Ther. 13 (2014) 2527–2536.
[29] A.M. Czarnecka, M. Kawecki, F. Lian, J. Korniluk, C. Szczylik, Feasibility, efficacy and safety of tyrosine kinase inhibitor treatment in hemodialyzed patients with renal cell cancer: 10 years of experience, Future Oncol. 11 (2015) 2267–2282.
[30] G. Sonpavde, T.E. Hutson, Pazopanib: a novel multitargeted tyrosine kinase inhibitor, Curr. Oncol. Rep. 9 (2007) 115–119.
[31] J.Y. Winum, A. Maresca, F. Carta, A. Scozzafava, C.T. Supuran, Polypharmacology of sulfonamides: pazopanib, a multitargeted receptor tyrosine kinase inhibitor in clinical use, potently inhibits several mammalian carbonic anhydrases, Chem. Commun. (Camb.) 48 (2012) 8177–8179.
[32] S.G. Kucukguzel, S. Senkardes, Recent advances in bioactive pyrazoles, Eur. J. Med. Chem. 97 (2015) 786–815.
[33] D. Raffa, B. Maggio, M.V. Raimondi, S. Cascioferro, F. Plescia, G. Cancemi, G. Daidone, Recent advanced in bioactive systems containing pyrazole fused with a five membered heterocycle, Eur. J. Med. Chem. 97 (2015) 732–746.
[34] M.M. Goldenberg, Celecoxib, a selective cyclooxygenase-2 inhibitor for the treatment of rheumatoid arthritis and osteoarthritis, Clin. Ther. 21 (1999) 1497–1513 discussion 1427-1498.
[35] P.L. McCormack, Celecoxib: a review of its use for symptomatic relief in the treatment of osteoarthritis, rheumatoid arthritis and ankylosing spondylitis, Drugs 71 (2011) 2457–2489.
[36] A.L. Hsu, T.T. Ching, D.S. Wang, X. Song, V.M. Rangnekar, C.S. Chen, The cyclooxygenase-2 inhibitor celecoxib induces apoptosis by blocking Akt activation in human prostate cancer cells independently of Bcl-2, J. Biol. Chem. 275 (2000) 11397–11403.
[37] A.T. Koki, J.L. Masferrer, Celecoxib: a specific COX-2 inhibitor with anticancer properties, Cancer Control. 9 (2002) 28–35.
[38] P.M. Forde, D.S. Ettinger, Targeted therapy for non-small-cell lung cancer: past, present and future, Expert Rev. Anticancer Ther. 13 (2013) 745–758.
[39] G. Greenfield, S. McPherson, K. Mills, M.F. McMullin, The ruxolitinib effect: understanding how molecular pathogenesis and epigenetic dysregulation impact therapeutic efficacy in myeloproliferative neoplasms, J. Transl. Med. 16 (2018) 360.
[40] T. Rogez-Florent, S. Meignan, C. Foulon, P. Six, A. Gros, C. Bal-Mahieu, C.T. Supuran, A. Scozzafava, R. Frederick, B. Masereel, P. Depreux, A. Lansiaux, J.F. Goossens, S. Gluszok, L. Goossens, New selective carbonic anhydrase IX inhibitors: synthesis and pharmacological evaluation of diarylpyrazole-benzenesulfonamides, Bioorg. Med. Chem. 21 (2013) 1451–1464.
[41] M.J. Uddin, B.C. Crews, K. Ghebreselasie, M.N. Tantawy, L.J. Marnett, [I]-Celecoxib analogues as SPECT tracers of cyclooxygenase-2 in inflammation, ACS Med. Chem. Lett. 2 (2011) 160–164.
[42] R.G. Khalifah, The carbon dioxide hydration activity of carbonic anhydrase. I. Stop-flow kinetic studies on the native human isoenzymes B and C, J. Biol. Chem. 246 (1971) 2561–2573.
[43] H. Sakagami, Y. Uesawa, M. Ishihara, H. Kagaya, T. Kanamoto, S. Terakubo, H. Nakashima, K. Takao, Y. Sugita, Quantitative structure-cytotoxicity relationship of oleoylamides, Anticancer Res. 35 (2015) 5341–5351.
[44] H.I. Gul, M. Tugrak, H. Sakagami, P. Taslimi, I. Gulcin, C.T. Supuran, Synthesis and bioactivity studies on new 4-(3-(4-Substitutedphenyl)-3a,4-dihydro-3H-indeno[1,2-c]pyrazol-2-yl) benzenesulfonamides, J. Enzyme Inhib. Med. Chem. 31 (2016) 1619–1624.
[45] E. Unluer, H.I. Gul, A. Demirtas, H. Sakagami, N. Umemura, M. Tanc, C. Kazaz, C.T. Supuran, Synthesis and bioactivity studies of 1-aryl-3-(2-hydroxyethylthio)-1-propanones, J. Enzyme Inhib. Med. Chem. 31 (2016) 105–109.
[46] C. Yamali, H.I. Gul, H. Sakagami, C.T. Supuran, Synthesis and bioactivities of halogen bearing phenolic chalcones and their corresponding bis Mannich bases, J. Enzyme Inhib. Med. Chem. 31 (2016) 125–131.
[47] H.I. Gul, E. Mete, S.E. Eren, H. Sakagami, C. Yamali, C.T. Supuran, Designing, synthesis and bioactivities of 4-[3-(4-hydroxyphenyl)-5-aryl-4,5-dihydro-pyrazol-1-yl]benzenesulfonamides, J. Enzyme Inhib. Med. Chem. 32 (2017) 169–175.
[48] H.I. Gul, C. Yamali, F. Yesilyurt, H. Sakagami, K. Kucukoglu, I. Gulcin, M. Gul, C.T. Supuran, Microwave-assisted synthesis and bioevaluation of new sulfonamides, J. Enzyme Inhib. Med. Chem. 32 (2017) 369–374.
[49] H. Sakagami, Y. Masuda, M. Tomomura, S. Yokose, Y. Uesawa, N. Ikezoe, D. Asahara, K. Takao, T. Kanamoto, S. Terakubo, H. Kagaya, H. Nakashima, Y. Sugita, Quantitative structure-cytotoxicity relationship of chalcones, Anticancer Res. 37 (2017) 1091–1098.
[50] H. Sakagami, N. Okudaira, Y. Masuda, O. Amano, S. Yokose, Y. Kanda, M. Suguro, T. Natori, H. Oizumi, T. Oizumi, Induction of apoptosis in human oral keratinocyte by doxorubicin, Anticancer Res. 37 (2017) 1023–1029.
[51] H.I. Gul, M. Tugrak, M. Gul, H. Sakagami, N. Umemura, B. Anil, Synthesis and cytotoxicities of new azafluorenones with apoptotic mechanism of action and cell cycle analysis, Anticancer Agents Med. Chem. 18 (2018) 1770–1778.
[52] C. Yamali, H.I. Gul, G. Gunesacar, H. Sakagami, N. Okudaira, Y. Uesawa, H. Kagaya, Cytotoxicity, apoptosis, and QSAR studies of phenothiazine derived methoxylated chalcones as anticancer drug candidates, Med. Chem. Res. 27 (2018) 2366–2378.
[53] D. Ozmen Ozgun, H.I. Gul, C. Yamali, H. Sakagami, I. Gulcin, M. Sukuroglu, C.T. Supuran, Synthesis and bioactivities of pyrazoline benzensulfonamides as carbonic anhydrase and acetylcholinesterase inhibitors with low cytotoxicity, Bioorg. Chem. 84 (2019) 511–517.
[54] S. Listl, L. Jansen, A. Stenzinger, K. Freier, K. Emrich, B. Holleczek, A. Katalinic, A. Gondos, H. Brenner, G.C.S.W. Group, Survival of patients with oral cavity cancer in Germany, PLoS ONE 8 (2013) e53415.
[55] N.T. Brockton, P. Lohavanichbutr, E.K. Enwere, M.P. Upton, E.N. Kornaga, S.C. Nakoneshny, P. Bose, C. Chen, J.C. Dort, Impact of tumoral carbonic anhydrase IX and Ki-67 expression on survival in oral squamous cell carcinoma patients, Oncol. Lett. 14 (2017) 5434–5442.
[56] A.W. Eckert, S. Horter, D. Bethmann, J. Kotrba, T. Kaune, S. Rot, M. Bache, U. Bilkenroth, W. Reich, T. Greither, C. Wickenhauser, D. Vordermark, H. Taubert, M. Kappler, Investigation of the prognostic role of carbonic anhydrase 9 (CAIX) of the cellular mRNA/Protein level or soluble CAIX protein in patients with oral squamous cell carcinoma, Int. J. Mol. Sci. 20 (2019) 375–392.
[57] M.H. Chien, T.H. Ying, Y.H. Hsieh, C.H. Lin, C.H. Shih, L.H. Wei, S.F. Yang, Tumor-associated carbonic anhydrase XII is linked to the growth of primary oral squamous

cell carcinoma and its poor prognosis, Oral Oncol. 48 (2012) 417–423.
[58] N.J. Beasley, C.C. Wykoff, P.H. Watson, R. Leek, H. Turley, K. Gatter, J. Pastorek, G.J. Cox, P. Ratcliffe, A.L. Harris, Carbonic anhydrase IX, an endogenous hypoxia marker, expression in head and neck squamous cell carcinoma and its relationship to hypoxia, necrosis, and microvessel density, Cancer Res. 61 (2001) 5262–5267.
[59] H.J. Shin, S.B. Rho, D.C. Jung, I.O. Han, E.S. Oh, J.Y. Kim, Carbonic anhydrase IX (CA9) modulates tumor-associated cell migration and invasion, J. Cell Sci. 124 (2011) 1077–1087.
[60] E. Svastova, S. Pastorekova, Carbonic anhydrase IX: a hypoxia-controlled "catalyst" of cell migration, Cell. Adh. Migr. 7 (2013) 226–231.
[61] C.A. Taft, V.B. Da Silva, C.H. Da Silva, Current topics in computer-aided drug design, J. Pharm. Sci. 97 (2008) 1089–1098, https://doi.org/10.1002/jps.21293.
[62] A. Ece, Towards more effective acetylcholinesterase inhibitors: a comprehensive modelling study based on human acetylcholinesterase protein–drug complex, J. Biomol. Struct. Dyn. 11 (2019) 1–8, https://doi.org/10.1080/07391102.2019.1583606.
[63] S. Biswas, R. McKenna, C.T. Supuran, Effect of incorporating a thiophene tail in the scaffold of acetazolamide on the inhibition of human carbonic anhydrase isoforms I, II, IX and XII, Bioorg. Med. Chem. Lett. 23 (2013) 5646–5649.
[64] A. Ece, e-Pharmacophore mapping combined with virtual screening and molecular docking to identify potent and selective inhibitors of P90 ribosomal S6 kinase (RSK), Turk. J. Pharm. Sci. 13 (2016) 241–248, https://doi.org/10.4274/tjps.28290.
[65] T.D. Penning, J.J. Talley, S.R. Bertenshaw, J.S. Carter, P.W. Collins, S. Docter, M.J. Graneto, L.F. Lee, J.W. Malecha, J.M. Miyashiro, R.S. Rogers, D.J. Rogier, S.S. Yu, E.G. AndersonGd, J.N. Burton, S.A. Cogburn, C.M. Gregory, W.E. Koboldt, K. Perkins, A.W. Seibert, Y.Y. Veenhuizen, P.C. Isakson Zhang, Synthesis and biological evaluation of the 1,5-diarylpyrazole class of cyclooxygenase-2 inhibitors: identification of 4-[5-(4-methylphenyl)-3-(trifluoromethyl)-1H-pyrazol-1-yl]benzenesulfonamide (SC-58635, celecoxib), J. Med. Chem. 40 (1997) 1347–1365.
[66] R. Di Santo, R. Costi, A. Roux, G. Miele, G.C. Crucitti, A. Iacovo, F. Rosi, A. Lavecchia, L. Marinelli, C. Di Giovanni, E. Novellino, L. Palmisano, M. Andreotti, R. Amici, C.M. Galluzzo, L. Nencioni, A.T. Palamara, Y. Pommier, C. Marchand, Novel quinolinonyl diketo acid derivatives as HIV-1 integrase inhibitors: design, synthesis, and biological activities, J. Med. Chem. 51 (2008) 4744–4750.
[67] R.V. Ragavan, V. Vijayakumar, N.S. Kumari, Synthesis and antimicrobial activities of novel 1,5-diaryl pyrazoles, Eur. J. Med. Chem. 45 (2010) 1173–1180.
[68] H.S. Ibrahim, S.M. Abou-Seri, M. Tanc, M.M. Elaasser, H.A. Abdel-Aziz, C.T. Supuran, Isatin-pyrazole benzenesulfonamide hybrids potently inhibit tumor-associated carbonic anhydrase isoforms IX and XII, Eur. J. Med. Chem. 103 (2015) 583–593.
[69] K.R.A. Abdellatif, E.K.A. Abdelall, W.A.A. Fadaly, G.M. Kamel, Synthesis, cyclooxygenase inhibition, anti-inflammatory evaluation and ulcerogenic liability of new 1,3,5-triarylpyrazoline and 1,5-diarylpyrazole derivatives as selective COX-2 inhibitors, Bioorg. Med. Chem. Lett. 26 (2016) 406–412.
[70] D.V.M. Laxmikant, S. Pavase, Kamalkishor G. Baheti, Anti-inflammatory exploration of sulfonamide containing diaryl pyrazoles with promising COX-2 selectivity and enhanced gastric safety profile, J. Het. Chem. 55 (2018) 913–922.
[71] G.M. Sheldrick, A short history of SHELX, Acta Crystallogr A 64 (2008) 112–122.
[72] Small-Molecule Drug Discovery Suite 2019-2, Schrödinger, LLC, New York, NY, 2019.
[73] Schrödinger Release 2019-2: Schrödinger Suite 2019-2 Protein Preparation Wizard; Epik, Schrödinger, LLC, New York, NY, 2016; Impact, Schrödinger, LLC, New York, NY, 2016; Prime, Schrödinger, LLC, New York, NY, 2019.
[74] G.M. Sastry, M. Adzhigirey, T. Day, R. Annabhimoju, W. Sherman, Protein and ligand preparation: parameters, protocols, and influence on virtual screening enrichments, J. Comput. Aided Mol. Des. 27 (2013) 221–234.
[75] Schrödinger Release 2019-2: LigPrep, Schrödinger, LLC, New York, NY, 2019.
[76] Schrödinger Release 2019-2: Glide, Schrödinger, LLC, New York, NY, 2019.
[77] R.A. Friesner, R.B. Murphy, M.P. Repasky, L.L. Frye, J.R. Greenwood, T.A. Halgren, P.C. Sanschagrin, D.T. Mainz, Extra precision glide: docking and scoring incorporating a model of hydrophobic enclosure for protein-ligand complexes, J. Med. Chem. 49 (2006) 6177–6196.
[78] H.I. Gul, Z. Yazici, M. Tanc, C.T. Supuran, Inhibitory effects of benzimidazole containing new phenolic Mannich bases on human carbonic anhydrase isoforms hCA I and II, J. Enzyme Inhib. Med. Chem. 31 (2016) 1540–1544.
[79] C. Yamali, M. Tugrak, H.I. Gul, M. Tanc, C.T. Supuran, The inhibitory effects of phenolic Mannich bases on carbonic anhydrase I and II isoenzymes, J. Enzyme Inhib. Med. Chem. 31 (2016) 1678–1681.
[80] K. Kantoh, M. Ono, Y. Nakamura, Y. Nakamura, K. Hashimoto, H. Sakagami, H. Wakabayashi, Hormetic and anti-radiation effects of tropolone-related compounds, In Vivo 24 (2010) 843–851.
[81] C. Yamali, H.I. Gul, D. Ozmen Ozgun, H. Sakagam, N. Umemura, C. Kazaz, M. Gul, Synthesis and cytotoxic activities of difluoro-dimethoxy chalcones, Anticancer Agents Med. Chem. 17 (2017) 1426–1433.
[82] M. Tugrak, C. Yamali, H. Sakagami, H.I. Gul, Synthesis of mono Mannich bases of 2-(4-hydroxybenzylidene)-2,3-dihydroinden-1-one and evaluation of their cytotoxicities, J. Enzyme Inhib. Med. Chem. 31 (2016) 818–823.
[83] K. Kucukoglu, F. Oral, T. Aydin, C. Yamali, O. Algul, H. Sakagami, I. Gulcin, C.T. Supuran, H.I. Gul, Synthesis, cytotoxicity and carbonic anhydrase inhibitory activities of new pyrazolines, J. Enzyme Inhib. Med. Chem. 31 (2016) 20–24.
[84] H. Inci Gul, C. Yamali, A. Tugce Yasa, E. Unluer, H. Sakagami, M. Tanc, C.T. Supuran, Carbonic anhydrase inhibition and cytotoxicity studies of Mannich base derivatives of thymol, J. Enzyme Inhib. Med. Chem. 31 (2016) 1375–1380.
[85] R. Suzuki, S. Matsuno, H. Sakagami, Y. Okada, Y. Shirataki, Search of new cytotoxic crude materials against human oral squamous cell carcinoma using ^{1}H NMR-based metabolomics, Anticancer Res. 34 (2014) 4117–4120.